AGU PUBLICATIONS

JGR

Journal of Geophysical Research: Oceans

RESEARCH ARTICLE

10.1002/2016JC012669

This article is a companion to Kessouri et al. [2017], https://doi.org/10.1002/2016JC012665.

Special Section:
Dense Water Formations in the North Western Mediterranean: From the Physical Forcings to the Biogeochemical Consequences

Vertical Mixing Effects on Phytoplankton Dynamics and Organic Carbon Export in the Western Mediterranean Sea

Faycal Kessouri[1,2,3], Caroline Ulses[1], Claude Estournel[1], Patrick Marsaleix[1], Fabrizio D'Ortenzio[4], Tatiana Severin[5,6], Vincent Taillandier[4], and Pascal Conan[6]

[1]Laboratoire d'aérologie, Université de Toulouse, CNRS, UPS, Toulouse, France, [2]Now at Department of Atmospheric and Oceanic Sciences, University of California, Los Angeles, CA, USA, [3]Also at Southern California Coastal Water Research Project, Costa Mesa, CA, USA, [4]Observatoire Océanologique, Sorbonne Universités, UPMC Université Paris 06, CNRS, Laboratoire d'océanographie de Villefranche (LOV), Villefranche-sur-Mer, France, [5]Marine Science Institute, University of Texas at Austin, Port Aransas, TX, USA, [6]Laboratoire d'Océanographie Microbienne (LOMIC), Observatoire Océanologique, Sorbonne Universités, CNRS, UPMC Univ Paris 06, CNRS, Banyuls/Mer, France

Abstract A 3-D high-resolution coupled hydrodynamic-biogeochemical model of the western Mediterranean was used to study phytoplankton dynamics and organic carbon export in three regions with contrasting vertical regimes, ranging from deep convection to a shallow mixed layer. One month after the initial increase in surface chlorophyll (caused by the erosion of the deep chlorophyll maximum), the autumnal bloom was triggered in all three regions by the upward flux of nutrients resulting from mixed layer deepening. In contrast, at the end of winter, the end of turbulent mixing favored the onset of the spring bloom in the deep convection region. Low grazing pressure allowed rapid phytoplankton growth during the bloom. Primary production in the shallow mixed layer region, the Algerian subbasin, was characterized by a long period (4 months) of sustained phytoplankton development, unlike the deep convection region where primary production was inhibited during 2 months in winter. Despite seasonal variations, annual primary production in all three regions is similar. In the deep convection region, total organic carbon export below the photic layer (150 m) and transfer to deep waters (800 m) was 5 and 8 times, respectively, higher than in the Algerian subbasin. Although some of the exported material will be injected back into the surface layer during the next convection event, lateral transport, and strong interannual variability of MLD in this region suggest that a significant amount of exported material is effectively sequestrated.

Key Points:
- Phytoplankton dynamics and organic carbon export are compared in three Mediterranean regions, differentiated by the mixed layer depth
- Despite a subpolar regime in the north and a subtropical regime in the south, annual primary production is similar in the studied regions
- Organic carbon export below 150 (800) m was 4–5 (3–8) times higher in convective regions than in the stratified region, in 2012/2013

Correspondence to:
F. Kessouri,
kesf@ucla.edu

Citation:
Kessouri, F., Ulses, C., Estournel, C., Marsaleix, P., D'Ortenzio, F., Severin, T., et al. (2018). Vertical mixing effects on phytoplankton dynamics and organic carbon export in the western Mediterranean Sea. *Journal of Geophysical Research: Oceans*, *123*, 1647–1669. https://doi.org/10.1002/2016JC012669

Received 28 DEC 2016
Accepted 3 JAN 2018
Accepted article online 19 JAN 2018
Published online 2 MAR 2018

1. Introduction

The mixed layer depth (MLD) is considered to be a major factor in controlling phytoplankton development (Sverdrup, 1953). At large scales, gyre circulation leads to surface waters being nutrient-rich over subpolar gyres, and nutrient-poor over subtropical gyres (Williams & Follows, 2003). The subpolar winter regime is characterized by a deepening of the mixed layer by several hundreds of meters and a large supply of inorganic nutrients in surface waters, while phytoplankton growth is limited by a lack of light when cells are transferred below the photic zone. In spring, an intense phytoplankton development occurs when the mixed layer shoals or, more generally, when turbulent mixing becomes weak (Taylor & Ferrari, 2011). This can be compared to the subtropical regime, where the deepening of the mixed layer to ~100 m, and phytoplankton growth cooccur. Under this regime, phytoplankton development is triggered by the mixing-induced supply of nutrients.

Export of organic carbon toward the deep ocean may play a determining role in sustaining mesopelagic ecosystems (Giering et al., 2017) and in sequestration of atmospheric carbon. This export exhibits large-scale variability in response to the variability of the MLD and plankton dynamics. Various authors have made satellite-based estimates of the global export due to biological pump (mainly driven by sinking of large particles produced in the euphotic layer [Buesseler, 2007b]), and pointed out high export under the photic zone in subpolar oceans, and low export in subtropical gyres (Henson et al., 2012; Laws et al., 2011; Siegel et al., 2014; Westberry et al., 2012). On the other hand, Gardner et al. (1995) suggested that the alternation between periods of stratification, favoring phytoplankton growth, and periods of mixed layer deepening enhances the efficiency of vertical export through the "mixed layer pump" process. This consists in

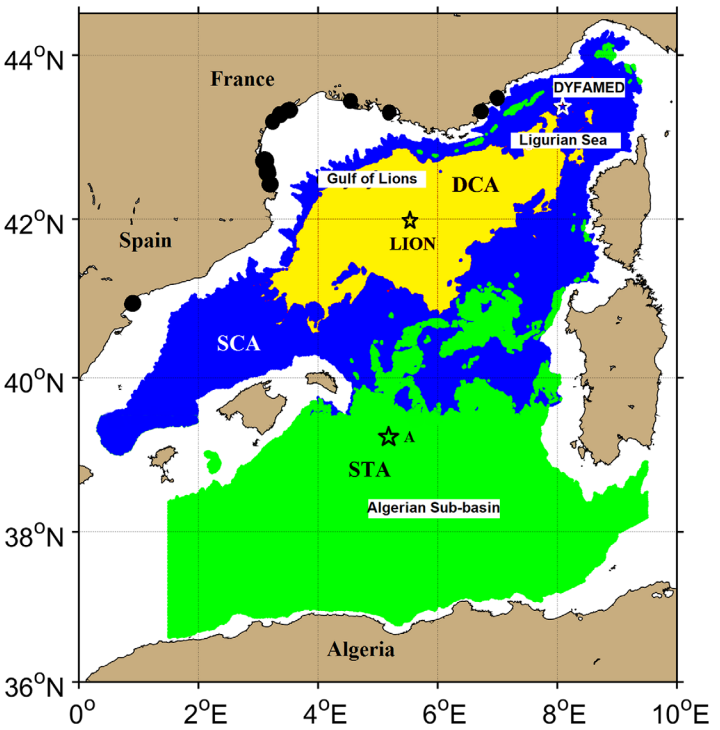

Figure 1. Location of the modeled area in the Western Mediterranean Sea. The colored regions correspond to the three regions considered in this study: the Deep Convection area (DCA, red), Shallow Convection area (SCA, blue), and Stratified area (STA, green).

increasing, through mixing, the slow sinking rate of phytoplankton and particles. Dall'Olmo et al. (2016) estimated that, in high latitudes, the ratio of mixed layer pump to biological pump is 23% on average, and can reach over 100%.

The western Mediterranean Sea (Figure 1) is characterized by the presence of subsurface water masses with high MLD gradients over several hundred kilometers in the south-north direction. Winter MLD values reach several hundred meters in the northwestern convection zone (Gulf of Lions), and only 60–80 m in the Algerian subbasin (Houpert et al., 2015). Furthermore, D'Ortenzio and Ribera d'Alcalà (2009) concluded that the western Mediterranean exhibits a bloom-like regime that is similar to the subpolar regime in its chlorophyll concentration and mixed layer seasonal evolution in the northwestern region, and a nonblooming behavior that is similar to the subtropical regime in the south.

Observational studies conducted in the western Mediterranean have shown that particulate organic carbon (POC) export fluxes below the euphotic layer and at middepth (1,000 m) are maximum during (February/March) and/or following winter mixing events (April, May, June) (3–4 times higher than the rest of the year; Gogou et al., 2014; Miquel et al., 2011; Stabholz et al., 2013). The authors of these studies argued that the spring peak is caused by fertilization induced by winter mixing, favoring a diatom-dominated ecosystem in the northwestern region. Moreover, Avril (2002) observed the transfer of dissolved organic carbon (DOC) at the surface to deep waters during intense vertical mixing in the northwestern region (DYFAMED station, Figure 1) and estimated that the winter mixing flux (10 gC m^{-2} yr^{-1}) constituted 91% of the annual flux at 100 m. Based on modeling studies, Ulses et al. (2016) found that the annual amount of exported organic carbon at 100 m depth is primarily related to the intensity of the deep convection process. They found that in years with strong convection, organic carbon export was twice that of years with shallow convection. Export efficiency showed the same interannual pattern, while the transfer to deep waters (>1,000 m) and the deposition on the seabed showed no clear trend. Bernardello et al. (2012) also used a modeling approach, and stressed the importance of the mixed layer pump in driving the interannual variability of POC export in the northwestern Mediterranean region. However, estimates of primary production and export flux remain uncertain in the western Mediterranean (Gogou et al., 2014) and, in general, for the global ocean (Henson et al., 2012; Siegel et al., 2014, 2016). Uncertainties in observational methods are mainly associated with the scarcity of measurements, which cannot reflect interannual and spatial variability. Other uncertainties arise from the lack of an overview of the system; for example, limited information is available on degradation and recycling processes (such as nitrification), and the contribution of DOC to total export. Estimates from modeling approaches, which simplify the system and are poorly constrained by sparse observations, are also associated with large uncertainties.

Modifications of water masses in the Mediterranean Sea have been observed since the 1990s and are now impacting the whole basin (Durrieu de Madron et al., 2011). Some have been partly attributed to climatic variations. For example, the Eastern Mediterranean Transient has been found to correspond to a switch in the region of deep water formation in the eastern Mediterranean, from the Adriatic to the Aegean (Roether et al., 1996), which produced a rise in the nutricline depth by 200–300 m (Klein et al., 1999). In the western Mediterranean, an acceleration of the increasing trend in salt and heat content in deep waters was reported following an intense dense water formation event in 2004/2005 (Borghini et al., 2014; Schroeder et al., 2008). It is, however, increasingly clear that climate change is already impacting water masses (Schroeder et al., 2016) and the ecosystem (Ben Rais Lasram et al., 2010). The Mediterranean Sea, which is characterized by a small spatial extent and mild meteorological conditions that facilitate the deployment of instruments at sea, is an excellent laboratory to monitor these impacts and to prepare models to predict future changes by calibrating them based on the present transition period.

The impacts of climate change may include the frequency and/or the intensity of convection, which could be modified as a result of increasing stratification in the upper layers (Somot et al., 2006). The weakening of convection processes could lead to a reduction in the occurrence and extent of phytoplankton blooms in the northwestern region. The consequences of climate change on the structure of the planktonic ecosystem and carbon sequestration require further examination. It is therefore a priority to better understand the functioning of the planktonic ecosystem, within both convection and stratified regions of the western Mediterranean, and assess how the ecosystem may evolve under weakened convection or in its absence.

In this context, and in the framework of the MerMex project, four cruises were carried out between July 2012 and June 2013 (Estournel et al., 2016b; Waldman et al., 2016). The data that were collected made it possible to describe the spatial distribution of phytoplankton in the deep convection northwestern Mediterranean during stratified, deep convection, and phytoplankton bloom periods (Mayot et al., 2017a; Severin et al., 2017). This unprecedented in situ observation offered a great opportunity to calibrate and validate a 3-D coupled physical-biogeochemical model (Estournel et al., 2016a; Kessouri et al., 2017). In the present study, we used this coupled model to investigate phytoplankton dynamics and the capacity of the western Mediterranean to export organic carbon below the photic layer and to transfer it to deep waters. We focused on the comparison of regions along a trophic and vertical mixing gradient encompassing the northern and southern regions. These regions are characterized by a similar distribution of nutrients, making it easier to discriminate the role of convection on primary production and export variability from other possible influences.

The article starts with a presentation of the methods and an evaluation of the model's results. The seasonal cycle of atmospheric forcing, MLD, and chlorophyll vertical profile are presented in sections 4.1 and 4.2. The seasonal cycle of primary production and carbon export is described in sections 4.3 and 4.4, respectively. Finally, the conditions favoring bloom onset, export of organic carbon under the photic zone, and its transfer to deep waters are discussed in section 5.

2. Methods

2.1. The Numerical Tool

A biogeochemical model was forced offline using the daily outputs of a 3-D hydrodynamic model. The models and their initial and boundary conditions are described in the following sections.

2.1.1. The Hydrodynamic Model

The SYMPHONIE model used in this study is a 3-D primitive equation, with a free surface and generalized sigma vertical coordinate, described in Marsaleix et al. (2008, 2009, 2011, 2012). This model was previously used in the Mediterranean to simulate open sea convection (Estournel et al., 2016a), and ocean circulation on the slope (Rubio et al., 2009) and on the continental shelf (Petrenko et al., 2008). The numerical domain (Figure 1) covered most of the western Mediterranean basin, using a curvilinear grid with variable horizontal resolution (Bentsen et al., 1999). The mesh size was 1.4 km to the south and 0.8 km to the north. The southward decrease in resolution was due to a compromise between the need to cover the western Mediterranean basin at a reasonable cost, while considering the northward decrease of the Rossby radius, and the need for increased resolution in the winter convection zone (Estournel et al., 2016a). Forty vertical levels were used with closer spacing near the surface (15 levels in the first 100 m in the center of the convection zone characterized by depths of ~2,500 m).

The model was initialized and forced at its lateral boundaries with daily analyses provided by the Mercator-Ocean operational system based on the NEMO model (Maraldi et al., 2013). The configuration of this model was the PSY2V2R4 prototype based on the NEMO ocean modeling platform and the SAM data assimilation system (Lellouche et al., 2013) at a resolution of 1/12° over the Atlantic and the Mediterranean from 20°S to 80°N. Following Estournel et al. (2016a), the initial field and open boundary conditions were corrected from stratification biases deduced from comparisons with observations taken during the MOOSE-GE cruise of August 2012. Atmospheric forcing (turbulent fluxes) was calculated using the bulk formulae of Large and Yeager (2009). Meteorological parameters including downward radiative fluxes were taken from the ECMWF (European Centre for Medium-Range Weather Forecasts) operational forecasts at 1/8° horizontal resolution and 3 h temporal resolution based on daily analyses at 00.00 UTC. River runoffs were considered based on

realistic daily values for French rivers (data provided by Banque Hydro, www.hydro.eaufrance.fr) and Ebro (data provided by SAIH Ebro, www.saihebro.com), and mean annual values for the other rivers.

2.1.2. The Biogeochemical Model

The Eco3M-S model is a multinutrient and multiplankton functional type model that simulates the dynamics of the biogeochemical decoupled cycles of several biogenic elements (carbon, nitrogen, phosphorus, and silicon), and of non-Redfieldian plankton groups. The model structure used in this study has been previously described in Ulses et al. (2016), Auger et al. (2011, 2014), and Herrmann et al. (2013). Most parameter values are based on the study of Ulses et al. (2016), but a new calibration was carried out for some parameters using several observational data sets (Kessouri et al., 2017).

The biogeochemical model was downscaled from the Mediterranean basin scale to the regional scale described here. The biogeochemical basin scale model was forced by the temperature, current, and vertical diffusivity daily fields of the NEMO model (PSY2V2R4 analyses), which was also used for the boundary conditions of our hydrodynamic model (section 2.1.1). This basin configuration was initialized in summer 2010, with climatological fields of nutrient observations from the oligotrophic period in the Medar/MedAtlas database (Manca et al., 2004). Daily values of all state variables were extracted from the basin-scale run for the initial and lateral boundary conditions of the regional model. This nesting protocol ensures the coherence of the physical and biogeochemical fields at the open boundaries. The regional model was initialized in August 2012. At the Rhone River mouth, nitrate, ammonium, phosphate, silicate, and DOC concentrations were prescribed using in situ daily data (P. Raimbault, personal communication, 2013). These data, combined with those of Moutin et al. (1998) and Sempéré et al. (2000), were used to estimate dissolved organic phosphorus and nitrogen, and particulate organic matter concentrations as described in Auger et al. (2011). At the other river mouths, climatological values were prescribed according to Ludwig et al. (2010). The deposition of organic and inorganic matter from the atmosphere was neglected in this study. Benthic fluxes of inorganic nutrients were considered by coupling the pelagic model with a simplified version of the metamodel described by Soetaert et al. (2001). The parameters of the latter model were set following the modeling study performed by Pastor et al. (2011) for the Gulf of Lions shelf.

2.2. MODIS Satellite Data Set

Daily mean surface chlorophyll concentrations were extracted from the MODIS (Moderate Resolution Imaging Spectroradiometer) Aqua (EOS PM) satellite data set (NASA Goddard Space Flight Center, Ocean Biology Processing Group, 2014) for the period September 2012 to September 2013, in order to evaluate the spatial and temporal variation of the modeled surface chlorophyll concentrations in the western Mediterranean.

2.3. Areas of Study

Temporal variations in the MLD are considered a major forcing of phytoplankton dynamics (Williams & Follows, 2003). In their study of the western Mediterranean, using a MLD data set and ocean color data, Lavigne et al. (2013) concluded that MLD plays a key role in phytoplankton phenology, and can explain the coexistence of the two trophic regimes previously observed (D'Ortenzio & Ribera d'Alcalà, 2009). A first regime in the northwestern convection region is characterized by a deepening of the mixed layer in winter (reaching 1,000 m for 52% of the years for which observations were available between 1980 and 2013; Somot et al., 2016), followed by an intense phytoplankton bloom (similar to the subpolar regime; Williams & Follows, 2003). A second regime in the southern (Algerian) subbasin is characterized by continuous slow phytoplankton growth, concomitant with the shallow deepening of the mixed layer (similar to the subtropical regime; Williams & Follows, 2003). By analyzing the interannual variability of satellite-derived surface chlorophyll, Mayot et al. (2016) distinguished two subregimes in the northwestern convection region: bloom was found to be more pronounced and delayed in the center of the convection zone than at its periphery. Mayot et al. (2017a) showed that these two subregimes are distinguished by the intensity and duration of the deepening of the mixed layer. Their study found that mean MLD exceeded 880 m for the central "high bloom" region, over a period of 1 month, and reached 475 m, for a couple of days, in the surrounding "bloom" region, in the winter of 2012/2013.

Following these earlier studies, we decided to divide the open-sea of the western Mediterranean (bathymetry $>$ 1500 m) into three regions (Figure 1), in order to carry out analyses of phytoplankton dynamics, and estimates of primary production and export. The first was the *Deep Convection* region, defined as the area where daily average of MLD exceeded 1,000 m for at least 1 day during the studied winter. The

second was the *Shallow Convection* region, defined as the area in which daily average of MLD exceeded 150 m but did not reach 1,000 m. The Shallow Convection region was located at the periphery of the first area and mostly covered the Balearic Sea. The third area, named the *Stratified* region, covered a large part of a deep pelagic zone in the southwestern Mediterranean (Algerian subbasin) where maximum winter MLD was less than 150 m. In the present study, MLD was defined as the depth where potential density exceeded the value at a depth of 10 m by 0.01 kg m^{-3} (Coppola et al., 2017). This density-based criterion (rather than a temperature-based criterion) avoids any overestimation of the MLD, and any consideration of surface restratification caused by a change in surface heat flux, especially in the deep convection region (Houpert et al., 2015). The division into regions allowed us to focus our analysis on the factors underlying differences in maximum winter MLD.

The heat fluxes, and hydrodynamic and biogeochemical variables that are presented in the following sections correspond to the values of these variables averaged over all model grid points included in the three areas. Furthermore, we calculated export below the regional maximum photic zone at 150 m. Following Lazzari et al. (2012), this estimate of the depth of the photic layer was based on the regional minimum value of the diffuse attenuation coefficient of light at 490 mm derived from satellite observations (http://marine.copernicus.eu/), found close to 0.03 m^{-1} over the study period, and on the Lambert-Beer formulation to evaluate photosynthetic available irradiance. Deep transfer was calculated at a depth of 800 m as, in general, temporal variability in water masses at depths $>$ 800 m is weak (Bethoux et al., 1989). Moreover, it is possible that, in convection regions, deep waters below 800 m are mixed with overlying waters, and a fraction of exported matter and its remineralization product are imported back into surface and intermediate layers during the following winters. To discuss deep transfer on a longer period than 1 year (section 5.4), we also estimated export below the maximum MLD, as recommended in Palevsky and Quay (2017): this was computed at the greatest depth between 800 m and the local maximum MLD over the study period, for each model grid point.

2.4. Determination of Bloom Onset

Understanding the environmental factors that control phytoplankton bloom onset has been a key issue in a large number of studies (Behrenfeld, 2010; Brody & Lozier, 2015; Henson et al., 2009; Siegel et al., 2002). Several methods have been defined to determine its date. Siegel et al. (2002) defined it as the first day of the year when surface chlorophyll concentration exceeds the annual median, plus 5%. Adjustments to this method have been made to capture the subtropical autumnal bloom, for instance, by considering the investigated year to start in September (Henson et al., 2009), or by avoiding consideration of a small, transient concentration increase by changing the value of the threshold (10% instead of 5%, as in Bernardello et al., 2012). Other studies (Behrenfeld, 2010; Brody & Lozier, 2015) used observational data to develop a method based on the net accumulation rate. The latter method is more appropriate to detect bloom onset when the phytoplankton biomass is initially low (Brody et al., 2013), as is the case in convective regions. In the present study, bloom onset was considered as the day on which the net accumulation rate of carbon biomass integrated through the water column (equation (1)) exceeded 50% of its annual maximum value.

$$r = \frac{Ln\ \frac{C(t+\Delta t)}{C(t)}}{\Delta t}, \tag{1}$$

where r is the net accumulation phytoplankton rate, $C(t)$ is the depth-integrated phytoplankton biomass, and $\Delta t = 7$ days. The index r was compared to an index based on surface chlorophyll, using the method of Siegel et al. (2002), that we adapted for our study, by considering that the year began in September.

3. Model Evaluation

A detailed validation of the coupled hydrodynamic and biogeochemical models over the study period is described in Estournel et al. (2016a) and Kessouri et al. (2017), respectively. Estournel et al. (2016a) conducted several comparisons with observations, such as the spatial distribution of water column stratification in winter at the scale of the northwestern subbasin (their Figure 6) or time series of the potential temperature profile in the center of the Gulf of Lions (their Figure 11). In Kessouri et al. (2017), a comparison of the biogeochemical model results with nutrients and chlorophyll concentrations measured during the DeWEx

winter and spring cruises was presented. This comparison showed that the model correctly reproduced the horizontal and vertical chlorophyll and nutrient distribution in these two seasons.

Here, the modeled seasonal evolution of surface chlorophyll in the three western Mediterranean regions (Deep Convection, Shallow Convection, and Stratified) is compared with that derived from MODIS data over the period September 2012 to September 2013 (Figure 2). Satellite data were interpolated on the model grid, then both modeled and observed chlorophyll were averaged in the three regions (model outputs corresponding to missing satellite data were not considered). Pearson correlations between surface modeled and satellite-derived chlorophyll concentrations were R = 0.8, 0.85, and 0.85 ($p < 0.01$) in the three regions, respectively (Figure 2, top plot). The Nash-Sutcliffe efficiency (NS = 0.61, 0.55, and 0.2, respectively), indicated good-to-excellent performance of the model according to Allen et al. (2002). Mean biases represented a percentage of the observed chlorophyll of −8% in the Deep Convection region, +16% in the Shallow Convection region,

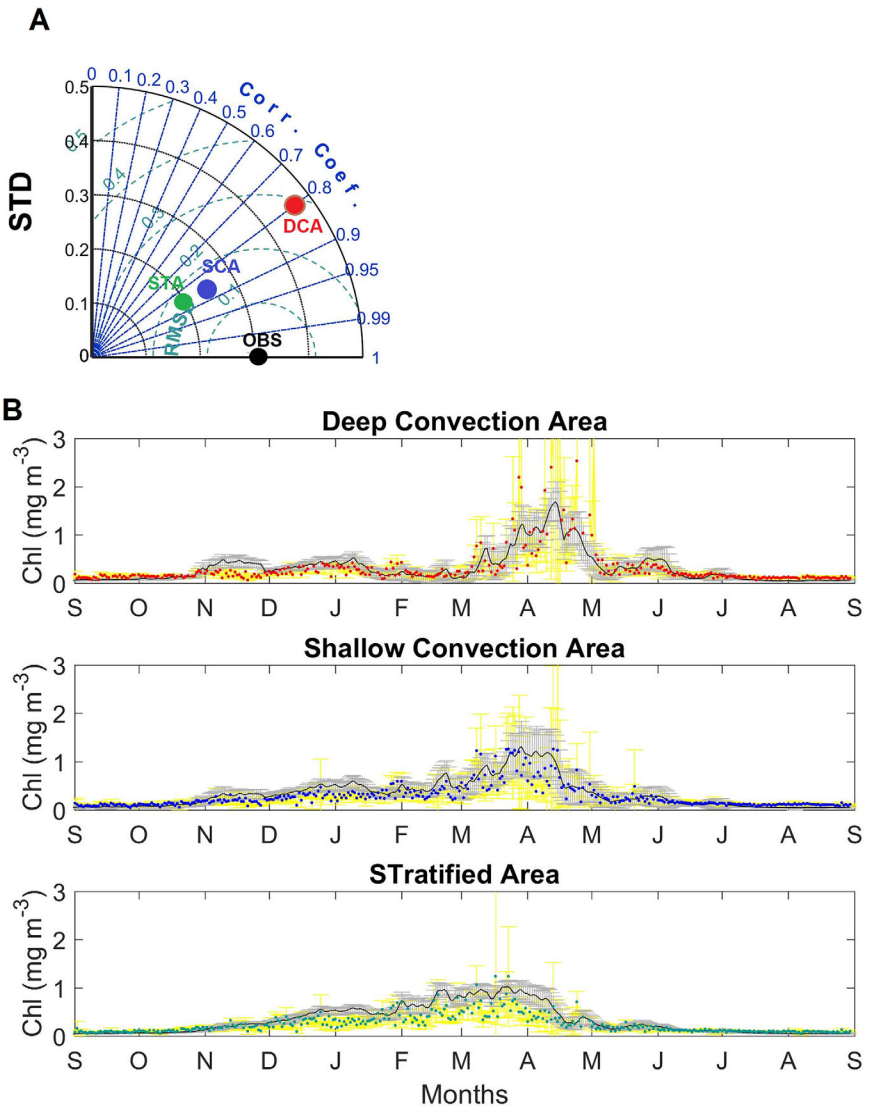

Figure 2. (top) Taylor diagram comparing the simulated and observed surface chlorophyll concentrations, where OBS indicates MODIS data and DCA, SCA, and STA indicate the model outputs in the Deep Convection region, Shallow Convection region, and Stratified region, respectively. (bottom) Time series of the simulated (black line, median; gray bar, standard deviation) and observed (colored points and colored blue bars for standard deviation) surface chlorophyll concentrations (in mg m^{-3}) in three western Mediterranean regions: the Deep Convection region (DCA, red points), Shallow Convection region (SCA, blue points), and Stratified region (STA, green points) from September 2012 to September 2013. The vertical dashed lines represent the dates of the blooms onset (see section 5.1 and Figure 6).

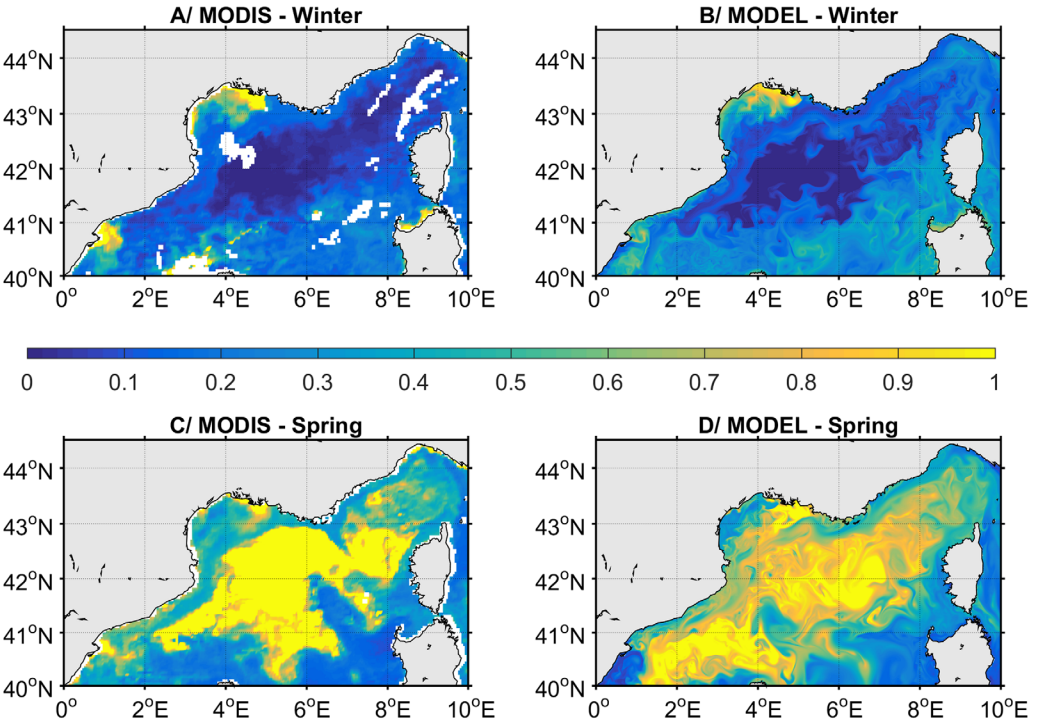

Figure 3. Comparison between the simulated and MODIS chlorophyll concentration (mg m^{-3}) in winter (19 February 2013, a and b) and spring (14 April 2013, c and d).

and +30% in the Stratified region. The temporal root mean square error was maximum (0.26 mg m^{-3}) in the Deep Convection area (Figure 2, top plot) where the signal was highly variable during bloom.

The timing of surface phytoplankton development and its magnitude were generally correctly represented by the model in the three studied regions. The observations and the model exhibited similar seasonal trends, that clearly show the contrast between the north and the south of the basin: in February, concentrations increased from north to south, while in April this trend was reversed. On the date of the maximum extent of the low chlorophyll area in the Deep Convection region (February 19 according to model outputs, cloud-free images were too scarce to confirm this), it covered the Gulf of Lions and Ligurian Sea (Figure 1) in both model results and observations (Figures 3a and 3b). The spatial pattern of surface chlorophyll during the period of maximum chlorophyll development (14 April) did not differ significantly between the model and observations ($R = 0.58$ [$p < 0.01$]) (Figures 3c and 3d). Spatial correlation in winter is higher $R = 0.8$.

Regarding the vertical distribution of chlorophyll in convection regions, Kessouri et al. (2017) found a good agreement between model results and DeWEx cruise observations. Moreover, the time evolution of the vertical distribution of phytoplankton in the Stratified (southern) region is consistent with climatological observations reported by Lavigne et al. (2015): the model correctly reproduces the formation of a deep chlorophyll maximum (DCM) after the winter mixing period and its deepening between 50 and 80 m in summer (presented in section 4.2).

The evaluation of the model indicates that it reproduced the annual cycle of surface chlorophyll concentration in the three studied regions. However, it was observed that it underestimated surface concentration in the Deep Convection region, and overestimated it in neighboring regions. Furthermore, the modeled vertical distribution was consistent with observations in the study area.

4. Results

4.1. Atmospheric Conditions

Intense cold and dry winds are an essential ingredient of deep convection. Using combined atmospheric and oceanic observations, Estournel et al. (2016b) showed restratification of the upper 500 m during periods

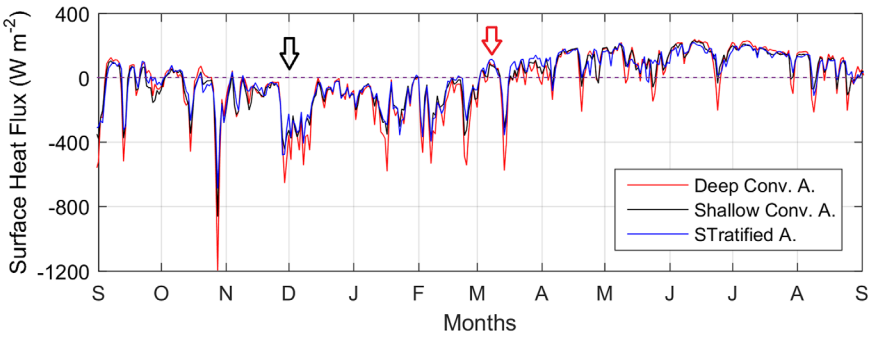

Figure 4. Time series of the spatially averaged heat flux (W m^{-2}) calculated for the three studied regions: Deep Convection area in red, Shallow Convection area in blue, and stratified area in green. The dates of the blooms onsets are indicated with arrows (see section 5.1).

of oceanic heat gain, generally associated with low wind conditions and, conversely, the destruction (within hours) of an ocean stratification in response to the passage of a continental air mass, associated with heat loss. Heat flux time series is therefore a relevant parameter to consider in explaining variation in the MLD, which impacts the availability of both nutrients and light for phytoplankton growth. A change in sign of surface heat fluxes can also be used to detect bloom onset, as it induces a decrease in turbulent mixing, increasing the time phytoplankton cells remain in the euphotic layer (Taylor & Ferrari, 2011).

The modeled heat flux evolution was similar in the three studied regions (Figure 4). Temporal correlation coefficients between heat fluxes in the Shallow Convection and Deep Convection regions, and between the Stratified and Deep Convection regions, were significant at 0.96 ($p < 0.01$) and 0.93 ($p < 0.01$), respectively. Each region was characterized by a major heat loss between September 2012 and mid-March 2013, and a heat gain from mid-March 2013 to September 2013. However, there were clear differences in its magnitude for the three regions. Specifically, heat losses were higher in the Deep Convection region, which is directly exposed to the Mistral and Tramontane winds, than in the two other regions. In this region, average of winter heat flux was -180 W m^{-2}, compared to -140 W m^{-2} in the Shallow Convection region and -130 W m^{-2} in the Stratified region. Heat loss exceeded 400 W m^{-2}, 11 times in the Deep Convection region from September 2012 to March 2013, while it only exceeded this value twice in the two other regions.

4.2. Temporal Variability of MLD and Chlorophyll Concentration

Figure 5 presents the time evolution of the modeled MLD, spatially averaged for the three regions. The mixed layer deepened progressively from October to January, and then more abruptly from January to March. Despite a few events, characterized by low surface heat loss, that interrupted this deepening, it reached maximum values of 1,900 m in the Deep Convection region, 260 m in the Shallow Convection region and 60 m in the Stratified region at the end of February. During the first week of March, which was characterized by positive surface fluxes, significant restratification due to surface and intermediate waters advection was observed (Estournel et al., 2016b). This led to mixed layer shoaling in the Deep and Shallow convection regions. However, this stratification was insufficient to withstand mid-March gusty winds, which further deepened the mixed layer. After this last deep mixing event, stratification became stable, marking the end of winter.

The three regions were broadly similar in terms of their chlorophyll dynamics, the exception being winter. A DCM was observed in spring, summer, and autumn in the three regions. DCM formation was earlier in the Stratified region (mid-April) than in the Shallow Convection (end of April) and in Deep Convection (May) regions. From its formation, DCM deepened until August, when it reached 60–70 m. In autumn, it became shallower as the light intensity reduced. Chlorophyll concentrations in the DCM decreased from the time of the DCM formation in spring, until its disappearance in November. An intense wind event and heat loss at the end of October deepened the mixed layer, which reached the DCM and led to its disappearance by dilution (discussed in section 5.1.1). During the second half of December, surface chlorophyll concentration increased considerably.

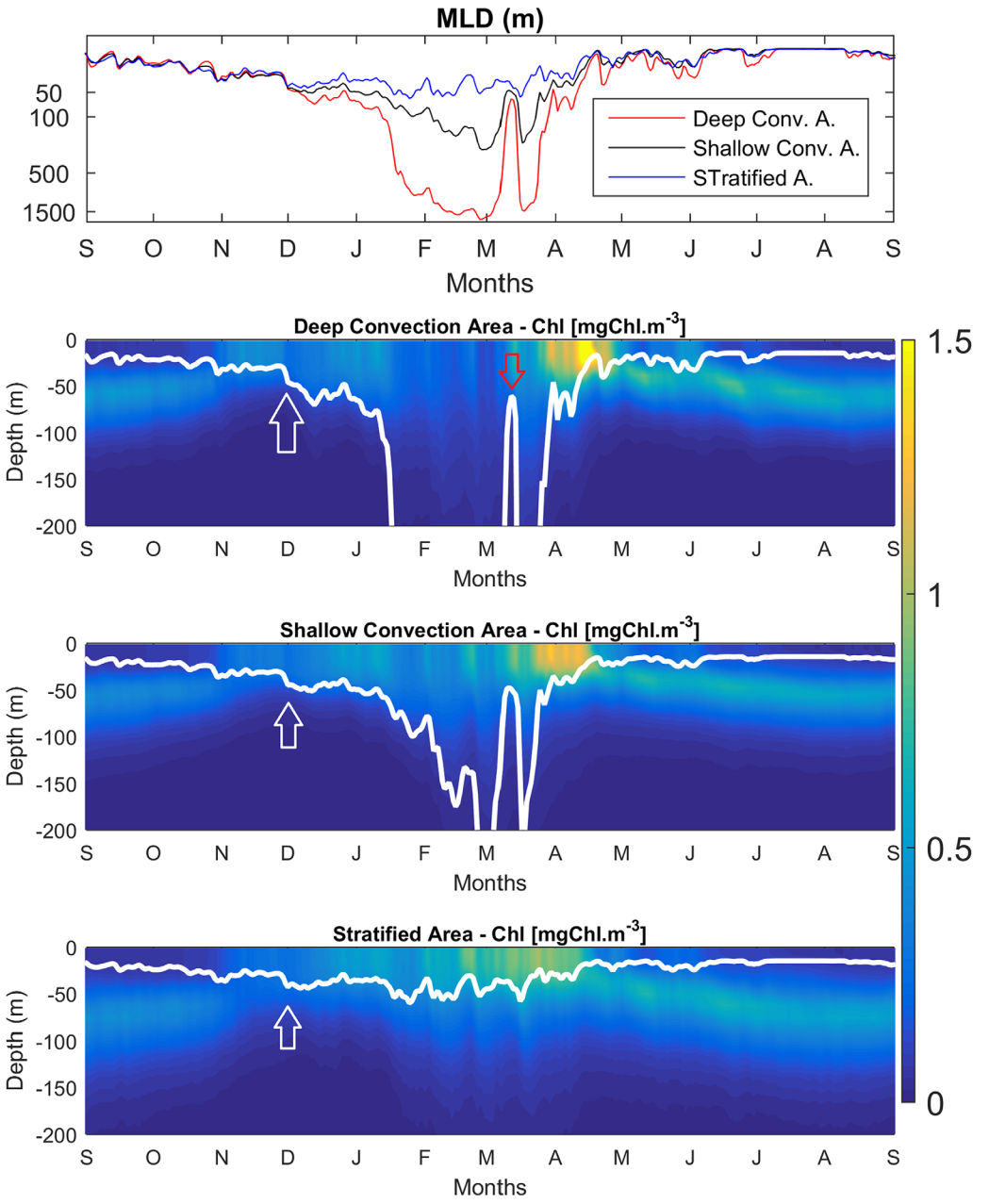

Figure 5. (top) The temporal evolution of the simulated MLD (m) in the Deep Convection region (black), the Shallow Convection region (blue), and the Stratified region (green) from September 2012 to September 2013. The *y* axis is logarithmic. The other plots represent the chlorophyll concentration (mg m^{-3}) averaged in each of the studied regions (Deep Convection region, Shallow Convection region, and Stratified region, from top to bottom plot, respectively). The MLD is superimposed (white line). Arrows indicate the bloom onsets (see section 5.1).

From mid-January to early March, several wind gusts interrupted surface phytoplankton development in all three regions, but the duration and frequency of these interruptions varied from one region to another. For example, in the Deep Convection region, surface chlorophyll concentrations decreased significantly in response to deep mixing, whereas in the Stratified region, the decrease was smaller and was concentrated into short periods (Figure 5). From the end of March to mid-April, all three regions were characterized by a sustained increase in surface chlorophyll concentration. A comparison of the regions suggests that strong mixing delayed the biomass increase (discussion in section 5.1). Moreover, surface phytoplankton development was shorter and more intense where mixing was deep. For instance, in the Deep Convection region, it

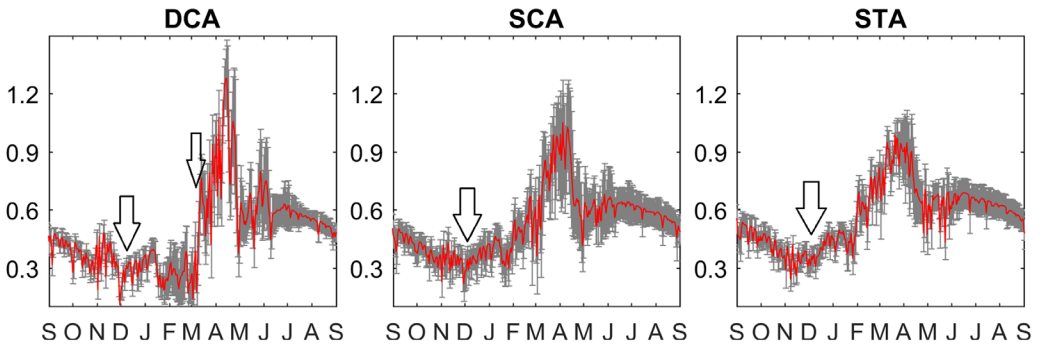

Figure 6. Time series from September 2012 to September 2013 of the simulated net primary production (NPP) (gC m^{-2} d^{-1}) spatially averaged (red) and standard deviation (grey) in the Deep Convection (DCA, left), Shallow Convection (SCA, middle), and Stratified (STA, right) regions. Vertical arrows indicate the blooms onset (See section 5.1).

lasted about 1.5 months with chlorophyll concentrations above 1.5 mg m^{-3} during the bloom. In the Stratified region, it lasted at least 2.5 months, with chlorophyll values remaining below 1 mg m^{-3}.

4.3. Primary Production

In winter (December–February), the modeled, vertically integrated net primary productivity (NPP, Figure 6) had a mean and standard deviation of 0.45 ± 0.09 and 0.55 ± 0.13 gC m^{-2} d^{-1} in the Shallow Convection and Stratified regions, respectively: both NPP means were higher than in the Deep Convection region (mean 0.3 gC m^{-2} d^{-1}). NPP increase began in February in the Shallow Convection and Stratified regions, and 1 month later in the Deep Convection region. NPP reached its maximum in all three regions in spring (mean ± standard deviation of 0.91 ± 0.21, 0.86 ± 0.13, and 0.8 ± 0.10 gC m^{-2} d^{-1} in the Deep Convection, Shallow Convection, and Stratified regions, respectively). A secondary peak (higher in the Deep Convection region than in the two other regions) occurred between mid-May and early June. From early June to November, NPP slowly decreased, with average values of 0.5 ± 0.05 gC m^{-2} d^{-1} in the three studied regions.

This seasonal evolution of NPP is consistent with earlier results based on in situ observations using the ^{14}C method in the Ligurian Sea (Marty & Chiavérini, 2002) and remote sensing in various regions of the Mediterranean basin (Bosc et al., 2004; Uitz et al., 2012). However, summer NPP was higher in the model (0.6 gC m^{-2} d^{-1}) than for satellite-based estimates (0.4 gC m^{-2} d^{-1}), in the Stratified region. This summer overestimation has also been identified for other numerical models (Allen et al., 2002; Crispi et al., 2002; Lazzari et al., 2012). These differences could be nuanced by limitations in the determination of primary production based on remote sensing in the presence of a DCM, as most of the light recorded by remote sensing emanates from the upper few centimeters of the water column (Helbling & Villafañe, 2009). The impact of this limitation on the estimate of annual primary production could be all the more significant following the work of Macias et al. (2014), who estimated that primary production in the DCM represents 62% of the total primary production in the open-sea Mediterranean regions. The results of our model showed that 90% of primary production in spring/summer, and 70% at the beginning of the fall occurred in the DCM layer in all three regions.

At the annual scale, we estimated a NPP of 175 ± 6 gC m^{-2} yr^{-1} in the Deep Convection region, 192 ± 14 gC m^{-2} yr^{-1} in the Shallow Convection region, and 207 ± 14 gC m^{-2} yr^{-1} in the Stratified region. Because of the overestimation of surface chlorophyll in the Stratified region, and the underestimate in the Deep Convection region, we did not consider the interregion NPP trend significant. By way of comparison, Lazzari et al. (2012) did not observe any clear NPP gradient between the eastern Algerian subbasin and the northwestern region, based on a coupled physical-biogeochemical model.

4.4. POC and DOC Export

Figure 7 presents the time evolution of the modeled export of DOC and POC at 150–800 m depths. This was calculated as the net downward flux induced by turbulent mixing, advection, and sedimentation (for particulate matter). In summer and autumn, vertical export was low in all three regions. In the Deep Convection region, where the MLD reached at least 500 m between mid-January and the first week of March

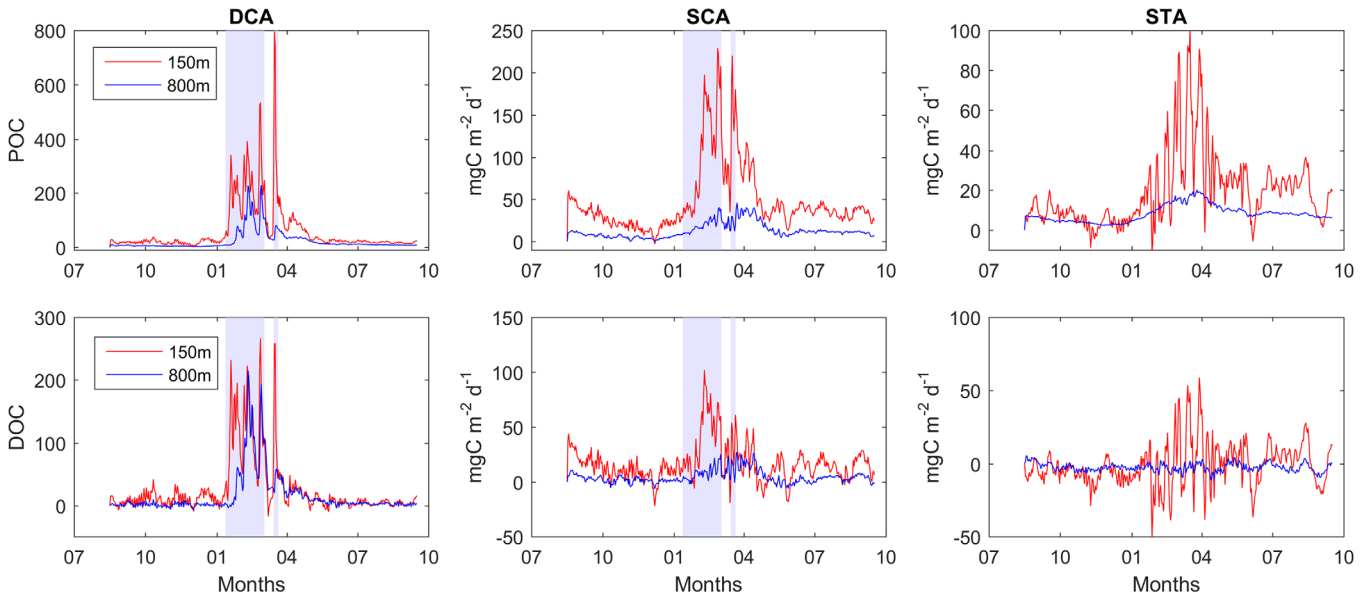

Figure 7. Time series from September 2012 to September 2013 of the modeled particulate (top plot) and dissolved (bottom plot) organic carbon export (mgC m^{-2} d^{-1}) at 150 m depth in red and 800 m in blue, in the Deep Convection Area (DCA, left), Shallow Convection Area (SCA, middle), and Stratified Area (STA, right). The first blue bar corresponds to the main convection event and the second blue bar represents the short deep mixing event of the third week of March.

(Figure 5), POC and DOC fluxes were strong and variable, with peaks coinciding with strong mixing events (mid-January, beginning, and end of February, and mid-March, see Figure 4). During the main convection event, the export at 150 (800) m reached 0.6 (0.2) gC m^{-2} d^{-1} for POC, and 0.25 (0.2) gC m^{-2} d^{-1} for DOC. During the secondary convection event (the third week of March), simulated export is characterized by a high peak at 150 m (0.95 gC m^{-2} d^{-1} for POC and 0.30 gC m^{-2} d^{-1} for DOC), with another moderate peak at 800 m (0.06 and 0.05 gC m^{-2} d^{-1} for POC and DOC, respectively). Similarly, in the Shallow Convection region, POC and DOC export was maximum during mixing events, exceeding 0.15 gC m^{-2} d^{-1} and 0.05 gC m^{-2} d^{-1}, respectively, at 150 m (compared to 0.02 gC m^{-2} d^{-1} and 0.02 gC m^{-2} d^{-1}, respectively, at 800 m). In both convection regions, an increase of POC and DOC export was simulated at 150 m in April during bloom. In the Stratified region, POC export at both depths was maximum during mixing periods, notably the period coinciding with maximum phytoplankton development (when it reached 0.10 and 0.02 gC m^{-2} d^{-1}). DOC export at 150 m was highly variable (positive and negative peaks reaching 0.05 gC m^{-2} d^{-1}), especially in winter; it was much lower at a depth of 800 m for the whole year.

Table 1
Annual Organic Carbon Export (gC m^{-2} yr^{-1}), and Export and Transfer Efficiency in Percentage From September 2012 to September 2013 at 150 and 800 m Depths, and at the Annual Maximum Depth Between 800 m and the Winter MLD (Noted max (800 m, MLD), See Definition in section 2.3)

	Deep convection	Shallow convection	Stratified
NPP 0–150 m	174	190	206
POC export at 150 m	24.8	15.4	8.1
DOC export at 150 m	10.0	4.5	−1.1
POC export at 800 m	7.8	4.2	3.4
DOC export at 800 m	5.4	1.5	−1.7
POC export at max (800 m, MLD)	1.4	4.2	3.4
DOC export at max (800 m, MLD)	0.1	1.5	−1.7
POC export at 150 m/NPP	14.3	8.1	3.9
POC export at 800 m/NPP	4.5	2.2	1.6
POC export at max (800 m, MLD)/NPP	0.8	2.2	1.6
OC export at 150 m/NPP	20.0	12.4	3.0
OC export at 800 m/NPP	7.6	3.0	0.8
OC export at max (800 m, MLD)/NPP	0.9	3.0	0.8
POC export at 800 m/POC export at 150 m	31.6	27.1	41.8
POC export at max (800 m, MLD)/ POC export at 150 m	5.6	27.1	41.8
OC export at 800 m/OC export at 150 m	38.1	28.7	23.6
OC export at max (800 m, MLD)/ OC export at 150 m	4.3	28.7	23.6

At the annual scale (Table 1), modeled POC and DOC export at both depths followed the same increasing trend: it was higher in regions where vertical mixing was deeper. The spatial mean and standard deviation of export at 150 (800) m were estimated at 25 ± 34 (8 ± 9), 15 ± 14 (4 ± 6), and 8 ± 6 (3 ± 4) gC m^{-2} yr^{-1} for POC, and 10 ± 17 (5 ± 7), 5 ± 6 (1 ± 1.5), and -1 ± 5 (-2 ± 3) gC m^{-2} yr^{-1} for DOC, in the Deep Convection, Shallow Convection, and Stratified regions, respectively. It is noteworthy that spatial variability was high within each region. The influence of convection on annual export will be discussed in section 5.2, and the efficiency of export and transfer to deep waters in section 5.3. The deep transfer of organic carbon and the comparison of the three regions on a decadal timescale will be discussed in section 5.4.

The simulated seasonal evolution of POC export below the photic zone agrees with sediment trap measurements from the DYFAMED station in the Ligurian Sea (Figure 1) (Miquel et al., 2011) and the LION site in the Gulf of Lions (Figure 1) (Stabholz et al., 2013). Both indicated: (1) rapid exports of particulate and dissolved matter during convection; (2) a bloom-induced export in spring; and (3) low export rates during the stratified period. From a quantitative point of view, Gogou et al. (2014) estimated an annual flux of 23 gC m^{-2} yr^{-1} at 100 m at the LION site (Figure1); Miquel et al. (2011) found an annual flux of 2.5 gC m^{-2} yr^{-1} at 200 m at DYFAMED; and Zúñiga et al. (2007) reported an annual flux of $\sim$6 gC m^{-2} yr^{-1} at 250 m in the Algerian subbasin (Point A on Figure 1). At the same locations and depths, our model estimated annual POC fluxes of 52, 19, and 11 gC m^{-2} yr^{-1}, respectively. The higher POC fluxes obtained in the convection regions in the model may be partly explained by an underestimation of POC export from sediment trap measurements during intense mixing periods (Buesseler et al., 2007). Regarding DOC export, our estimate of 18 gC m^{-2} yr^{-1} is similar to measurements carried out by Copin-Montégut and Avril (1993) and Avril (2002) of 18 and 12 $\pm$ 6 gC m^{-2} yr^{-1}, respectively, at 100 m in the Ligurian Sea. The annual POC flux at mid-depth has been estimated in observational studies at the LION site as 2.4 and 1.9 gC m^{-2} yr^{-1} at 1,000 m (Gogou et al., 2014; Stabholz et al., 2013). This can be compared to 1.6 gC m^{-2} yr^{-1} at 1,000 m at DYFAMED (Miquel et al., 2011), and 4.8 gC m^{-2} yr^{-1} at 845 m in the Algerian subbasin (Zúñiga et al., 2007). At the same locations and depths, the model computed sedimentation export of 2.8, 2.6, and 3.1 gC m^{-2} yr^{-1}, respectively, which is close to observations.

5. Discussion

5.1. Conditions Favoring Bloom Onset

5.1.1. Autumnal Bloom

As described in section 2.4, we determined bloom onset based on the net accumulation rate of phytoplankton biomass. The autumnal bloom onset occurred at the beginning of December in the two convective regions, and a few days later in the Stratified region (red vertical dashed lines in Figure 8). This difference is not significant, as it is sensitive to the choice of the threshold for the rate of accumulation (especially in the Stratified region). The following analysis concerns the early December period for the three regions.

Atmospheric forcing, biotic, and abiotic conditions at the onset of the autumnal bloom were similar in the three regions: (1) bloom was triggered during a period of high heat losses (Figures 8b, 8h, 8n); (2) the mixed layer suddenly deepened (40–50 m in the three regions, Figures 8c, 8i, 8o); (3) turbulent diffusivity suddenly increased in all regions (Figures 8d, 8j, 8p); (4) zooplankton integrated biomass constantly decreased after September (Figures 8e, 8k, 8q); and (5) nitrate and phosphate concentrations at the surface began to increase in all regions: concentrations reached 2 and $>$ 0.1 mmol m^{-3}, respectively, in the Deep Convection region, about 2 times lower in the Shallow Convection region, and 4 times lower in the Stratified region, while they had been close to 0 prior to the bloom triggering (Figures 8f, 8l, 8r).

An estimate of bloom onset based on surface chlorophyll, rather than vertically integrated organic carbon would have brought it forward by 1 month (Figure 8, dashed black lines). The increase of surface chlorophyll at the end of October was caused by the erosion of the DCM, at a time when the mixed layer deepened, without reaching the nutricline. This purely physical process was not accompanied by an increase in integrated carbon (red solid line in Figures 8a, 8g, 8m) and was therefore, not considered as bloom within the meaning of integrated biomass increase. It should be noted that the corollary of this process is a potential bias in remote sensing detection of post-DCM bloom. The period between the two estimates (based on surface chlorophyll and vertically integrated biomass) corresponds to the increase in the MLD from the DCM to the nutricline. In our case, this period lasted 1 month, which appears long if we consider the proximity of the DCM to the nutricline (about 20 m, see Kessouri et al., 2017). However, in the present case, it corresponded to the period between two strong wind and heat loss events at the end of October and the end of November (Figure 4), each of which coincided with a sudden deepening of the mixed layer (see Estournel et al., 2016a, their Figure 11 for the temperature evolution in the 150 m upper layer). The first event deepened the mixed layer down to the DCM, and the second brought it below the nutricline. This sequence of events, which began with the mixing of the DCM, followed by an increase of primary production caused by the nutrient supply from deeper layers, induced by increased wind stress, has been previously described by Chiswell et al. (2013). Lavigne et al. (2015) indicated that DCM erosion could explain 60% of chlorophyll profiles observed in the Ionian region in December and January.

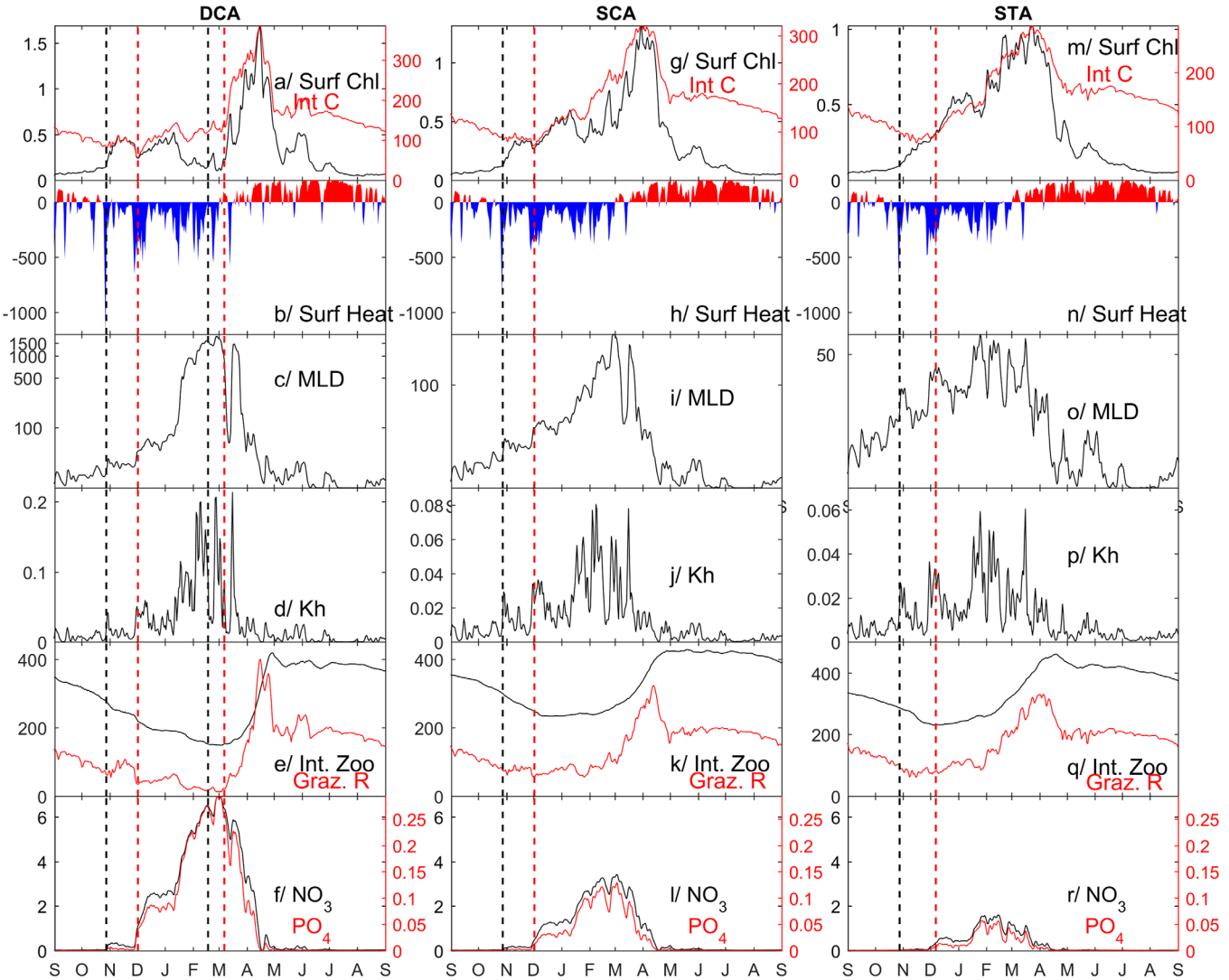

Figure 8. Time series from September 2012 to September 2013 of (a, g, m) modeled depth-integrated phytoplankton biomass (mgC m^{-2}) in red and surface chlorophyll concentration (mmol m^{-3}) in black, (b, h, n) net heat flux (W m^{-2}) with heat losses in blue and heat gains in red, (c, i, o) MLD (m), (d, j, p) the 0–75 m averaged turbulent diffusivity (m^2 s^{-1}), (e, k, q) depth-integrated zooplankton biomass in black (mgC m^{-2}) and grazing rate in red (mgC m^{-2} d^{-1}), and (f, l, r) nitrate (in black) and phosphate (in red) surface concentrations (mmol m^{-3}), in the Deep Convection area (DCA, left), the Shallow Convection area (SCA, middle), and the Stratified area (STA, right). Vertical dashed lines indicate the dates of the bloom onsets (black = using surface chlorophyll, red = using the vertically integrated biomass).

The triggering of the autumn bloom corresponds to the description by Williams and Follows (2003) of the subtropical bloom onset, which occurs when the deepening mixed layer provides new nutrients (Figure 9). However, we noted that the integrated zooplankton biomass was low in all three regions at autumn bloom onset (reaching a minimum in the Shallow Convection and Stratified regions). Therefore, it is likely that the low magnitude of grazing pressure participated to trigger the autumn bloom (Behrenfeld, 2010; Behrenfeld & Boss, 2014). Moreover, we noted that the ongoing mixed layer deepening following the autumn bloom induced dilution, which prevented the zooplankton biomass taking advantage of the autumn bloom to grow in the Deep Convection region.

5.1.2. Winter/Early Spring Bloom in the Deep Convection Area

In the Deep Convection region, the autumnal bloom was interrupted for a period of 2 months (from mid-January to mid-March) due to a lack of light that was, in turn, due to deep mixing. In February, the patch of chlorophyll was vertically homogeneous with a surface chlorophyll concentration below 0.1 mg Chl m^{-3} (Figures 3a and 5a) and high nutrient concentrations (>7 mmol N m^{-3} and > 0.3 mmol P m^{-3}) (Kessouri

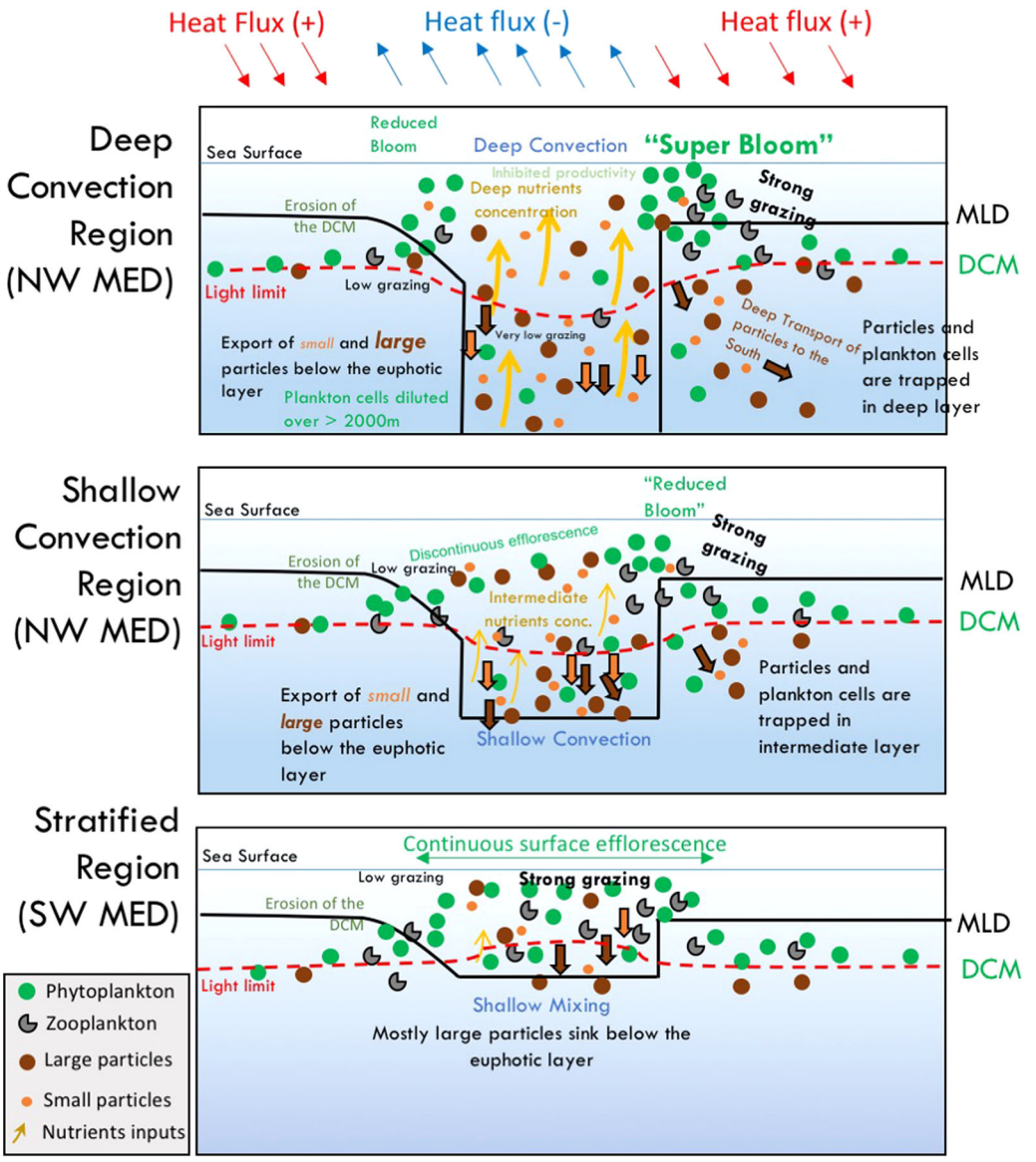

Figure 9. A conceptual model representing plankton growth and particles export for three different vertical mixing regimes in the western Mediterranean Sea. A first (autumnal) bloom was triggered by the injection of nutrients into the euphotic layer when mixed layer deepened in the three regions. The efflorescence was continuous in the stratified region during the mixing period, whereas it was interrupted in the convection regions due to mixing-induced light deficit. In convection regions, a second (spring) bloom occurred under low grazing pressure and decreasing mixed layer depth condition. After the mixing period, a deep chlorophyll maximum reformed in the three regions. Material exported below the euphotic layer was mostly composed of fast sinking particles in the stratified region. In the deep convection region, vertical advection and mixing induced an increase of the relative contribution of slow particles, when compared to the stratified region. The lateral transports toward the Algerian subbasin prior the next convection event suggest a sequestration of a part of the material exported below the euphotic layer in deep convection region.

et al., 2017). The vertically integrated phytoplanktonic biomass was almost constant (Figure 8a). Winter/early spring bloom onset was identified in the Deep Convection region on 8 March. The conditions that triggered it differed from those that triggered autumnal bloom. Specifically, the former started after a few days of positive heat flux (Figure 8b), when vertical turbulence decreased significantly (Figure 8d), and the mixed layer became abruptly shallower (100 m, Figure 8c). Nitrate and phosphate surface concentrations were high, with values >6.5 and >0.25 mmol m^{-3}, respectively (Figure 8f), while zooplankton biomass and grazing rate reached their annual minimum (Figure 8e).

These results (summarized in Figure 9) are consistent with the analysis of the triggering of the North Atlantic subpolar bloom by Williams and Follows (2003), and the results of Taylor and Ferrari (2011) obtained from analytical theory and high-resolution numerical simulations. Both studies emphasized the role of positive (or the reduction of negative) surface heat fluxes. The simultaneous breakdown of turbulence and a decrease in MLD means that our results also support the discussion of Brody et al. (2013), who argued that a change in sign of heat flux is not the only factor that could restratify the mixed layer, horizontal advection being another. For example, restratification could occur in response to horizontal advection by mixed layer eddies, as shown by Mahadevan et al. (2012), based on observations in the North Atlantic.

The work of Estournel et al. (2016a) showed that, based on a heat and salt budget in the convection zone, from December, horizontal advection acted to stratify the surface layer, with a sustained warming trend that opposed the effect of surface heat fluxes. They reported that during a period of light winds (the beginning of March), the heat budget became positive in surface and intermediate layers. This was argued to be due to the fact that the front between the convective dense layer and adjacent light water became baroclinically unstable, producing restratification by advection of warm water inside the mixed patch.

Following these authors, it is clear that restratification is intrinsically linked to the change in sign of surface fluxes (or the fall of negative fluxes) as baroclinic instability develops when surface heat losses decrease and no longer maintain the verticality of isopycnals. This suggests that the bloom was indirectly triggered by the decline in surface heat losses, which induced a conjunction of closely related effects: the breakdown of turbulence and water column restratification. However, it should be noted that these arguments were based on a spatial average over a relatively wide, and very heterogeneous area. It is probable that if each point of the model is examined, processes would be more differentiated. For example, the main impact of restratification induced by frontal instabilities should have been at the perimeter of the domain, whereas the 1-D turbulence breakdown process was probably more effective in the center of the convective patch. Although a study of these coupled, submesoscale processes is beyond the scope of this paper, it deserves dedicated examination.

Our results also illustrate that the decoupling of phytoplankton and grazers during the winter period was another factor that favored phytoplankton growth after bloom onset. It is of note that small positive and negative changes in the integrated phytoplankton biomass in winter (from December to the spring bloom onset) were associated with the beginning and end of windy conditions and induced heat flux, and uncorrelated with variations in grazing pressure. This indicates that prey-predator decoupling was strong throughout the winter (phytoplankton development being mostly related to mixing-induced nutrient supply). As Behrenfeld and Boss (2014) describe, recoupling is slow, as phytoplanktonic concentration must increase to stimulate grazing and encourage a subsequent increase in herbivores. This recoupling condition was not met during winter, and this explains the continuous decrease of zooplanktonic biomass, which only recovered when phytoplankton rapidly accumulated during the spring bloom as a result of the hydrodynamic factors discussed above.

Our results for the northwestern Mediterranean are consistent with those of Bernardello et al. (2012), who found that bloom started as vertical mixing decreased, generally in mid-March. They are also consistent with an observational study by D'Ortenzio et al. (2014) who reported that, in the deep convection region, the triggering of the bloom was unrelated to a change in the nutrient stocks of the euphotic layer since this stock was already available 3 months before onset. Finally, Auger et al. (2014) found a negative correlation between convection intensity and winter zooplankton biomass; this finding confirms the hypothesis that phytoplankton zooplankton decoupling induced by convection favors the explosion of the phytoplankton biomass.

5.1.3. Phytoplankton Growth in the Shallow Convection and Stratified Regions

In the Stratified region, no new bloom onset was identified during the months that followed the autumn bloom, while the vertically integrated biomass progressively increased. This is a characteristic of the subtropical region. In our results, after the autumn bloom, sustained winter mixing supplied nutrients almost continuously, producing a moderate accumulation of phytoplankton that was controlled by herbivores whose biomass was low, but which remained at a higher level than in the Deep Convection region.

The method based on accumulation rates identified several blooms in the Shallow Convection region in winter (not shown). Biomass increases corresponded to short, calm periods (heat gain or low heat loss), and

were followed by long periods of slow growth that resembled those of the Stratified region. It is likely that this behavior was specific to the particular year studied. Indeed, during the study period, the mixed layer remained relatively undeveloped for a long time, not exceeding 150 m in depth until the end of February (Figure 8i). Finally, findings for the Shallow Convection region lay between the other two regions (Figure 9). Like the Stratified region, the increase in integrated biomass was progressive but, like the Deep Convection region, surface chlorophyll increased rapidly in March/April. The grazing time series was more similar to that of the Stratified region than the Deep Convection region.

5.2. Influence of Convective Mixing on Organic Carbon Export

Organic carbon is exported under the productive layer through two main mechanisms: (1) sedimentation, which only involves individual or aggregated particles with a sufficiently high settling velocity compared to their rate of decomposition and remineralization; and (2) vertical mixing and advection that affect all organic carbon. Observations of the DeWEx Leg1 campaign in February 2013 showed the presence of phytoplankton at depths $>$ 2,000 m, at concentrations of 0.16 mg m^{-3} (Kessouri et al., 2017). These observations suggest that vertical mixing and advection are responsible for the presence of organic carbon, including light cells and detritus, in deep layers, as observed by Giering et al. (2017) in the Iceland Basin, and modeled by Ulses et al. (2016) in the northwestern Mediterranean. It is likely that a fraction of the exported matter observed in deep waters during the winter of 2012/2013 was permanently trapped when mixing stopped.

Our model reproduces the homogenization of chlorophyll throughout the mixed layer during convective events, shown by a comparison of the model's results with DeWEx cruise observations performed by Kessouri et al. (2017; see their Figure 3). Our findings show that the net export fluxes of POC and DOC at 150 m are more than 6 times higher during these events than during the rest of the year (Figure 7). The first convection event (15 January to 7 March) took place after the autumnal bloom (section 5.1). In the Deep Convection region, POC and DOC exports during this event constituted 48 and 61%, respectively, at 150 m, and 50 and 66%, respectively, at 800 m, of the annual amount. The percentages were lower in the Shallow Convection region: 32% and 39% for the export of POC and DOC, respectively, at 150 m (21 and 24%, respectively, at 800 m).

The secondary convection episode lasted 9 days, from 15 to 23 March 2013, and followed a period of weak stratification during which the winter/early spring bloom began (section 5.1). In the Deep Convection region, the export of POC and DOC integrated on this secondary event represented 12 and 9% at 150 m (6 and 7% at 800 m) of the respective annual export. This can be compared to the Shallow Convection region, with 8 and 6% at 150 m (6 and 11% at 800 m).

Intermittent convection was observed by Houpert et al. (2016) based on mooring data in the center of the Gulf of Lions, with a secondary deep convection event occurring in March, each year from 2009 to 2013. The model revealed the importance of this recurrent characteristic on the annual export of organic matter. It appears an alternation of periods of restratification, that favors phytoplankton growth, and vertical mixing, that entrains a fraction of new biomass under the euphotic layer. This phenomenon could explain the different peaks in POC and DOC export modeled in mid-January, the beginning, and end of February, and the third week of March in convection regions. These peaks corresponded to peaks in heat loss at the ocean surface (Figure 4) that triggered convection.

The importance of this "mixed layer pump" mechanism (Gardner et al., 1995), which is very clear in the present study period, has been reported in other studies. Bernardello et al. (2012) showed that the frequency of gales during the bloom period was a determining factor in the interannual variability of export in the deep convection region of the northwestern Mediterranean. In other regions, Bishop et al. (1986) estimated that 67% of primary produced carbon was removed by convective mixing during a transient stratification period in a warm-core ring in the northwest Atlantic. Similarly, Ho and Marra (1994) found that a large amount of newly produced organic carbon was exported by mixing during a transient stratification period in the northeast Atlantic. In their study of a shallow convection region in the North Atlantic and equatorial Pacific, Gardner et al. (1995) reported the importance of the deepening of the mixed layer at night, which favored the new production during the day and export of organic carbon produced. Koeve et al. (2001) estimated that vertical mixing associated with storms, which interrupted the beginning of the early spring

bloom, contributed to the export of a large fraction of seasonal new production (between 56 and 65% in 1992, and about 36% in 1989) in the northeast Atlantic.

5.3. Efficiency of the Export of Organic Carbon and Transfer to the Deep Layer

Table 1 presents the annual efficiency of the export of organic carbon produced in the surface layer, and its transfer to deep layers in the three study regions. We calculated the efficiency of organic carbon export as the ratio of the net export at 150 m to the depth-integrated NPP. The efficiency of organic carbon transfer to deep waters was defined as the ratio of net export at 800 m to net export at 150 m.

Since the modeled annual NPP showed no significant differences between the three regions (section 4.3), the overall efficiency of organic carbon export followed the same trend as exports at 150 m: it was higher in deep mixing regions (Table 1). Furthermore, a similar spatial pattern was found for the ratio of the net export of organic carbon at 800 m to the depth-integrated NPP. No clear trend was found for the fraction of organic carbon exported below 150 m that was also exported below 800 m; the only notable observation was that the highest value was found in the Stratified region.

Henson et al. (2012) estimated that the large-scale efficiency of organic carbon transfer to the deep ocean is opposite to the export efficiency; specifically, export efficiency is high (and transfer efficiency low) at high latitudes, while the opposite is found at low latitudes. The authors suggest that spatial variability in transfer efficiency can be explained by the structure of the ecosystem. At high latitudes, a diatom-dominated ecosystem favors export efficiency; material that is exported below the euphotic is labile and substantially degraded in the mesopelagic zone, leading to a poor deep transfer efficiency. At low latitudes, due to extensive recycling in the euphotic layer, more refractory organic matter is exported under the euphotic layer, favoring deep transfer efficiency. In our simulation, in the Stratified region, export at 150 m was dominated by the sedimentation of fast sinking organic particles (78%), a large proportion of which eventually reached deep waters. In convection regions, organic carbon was mainly exported by vertical motion, meaning that it was mostly composed of slow sinking particles (fast sinking particles represented 27% of the POC export at 150 m in the Deep Convection region). Higher transfer efficiency in the Deep Convection region compared to the Shallow Convection region could then be explained by the deeper mixed layer. On the one hand, intensified vertical mechanical mixing supported deep transfer. On the other hand, in the Shallow Convection region, a fraction of slow sinking particles that were exported at intermediate depths were remineralized before reaching 800 m, as Henson et al. (2012) suggest for low-latitude regions.

Our analysis of the DOC and POC contribution to the export at 150 and 800 m depths showed that the POC export dominated total organic carbon export in the three regions (Figure 7, Table 1). Our estimation of the DOC contribution to total export in convection regions (28.7% in the Deep Convection region, 22.5% in the Shallow Convection region) is close to the estimate of 20% by Hansell and Carlson (1998) for the global ocean. The DOC net flux at 150 m increased the efficiency of organic carbon export in convective regions (by more than 25%), while its contribution was negative (–30%) in the Stratified region. The increasing contribution of DOC to total export in stronger mixing regions was consistent with the fact that DOC was only exported toward the bottom by turbulent mixing and vertical advection in the model, while POC was also exported by sedimentation. The export of POC by sedimentation occurred throughout the year. Ulses et al. (2016) used the same coupled model in the northwestern Mediterranean deep convection region, and found the contribution of sedimentation export to total export ranged from 20 to 34%, with a maximum linked to the spring bloom in April/May. In contrast, we found that DOC export under the euphotic layer was very low outside the winter mixing period, and in downwelling zones (continental slope, mesoscale vortices). As a consequence, DOC accumulated in the surface layer during the stratified period, as observed by Avril (2002) and modeled by Guyennon et al. (2015).

Consistent with the study of Giering et al. (2017) and Dall'Olmo et al. (2016), our results suggest that regions characterized by a clear deepening of the mixed layer may be characterized by a high export of organic carbon toward deep waters. The supply of organic carbon under the photic zone could constitute an important food source for organisms that inhabit the mesopelagic zone.

5.4. Potential Implications on Carbon Sequestration

The role of convection regions in terms of carbon sequestration efficiency is unclear, due to the counteracting effects of convective mixing. These effects are characterized by, on the one hand, an increased export of organic carbon under the euphotic layer and, on the other hand, the supply in the surface layer of dissolved

inorganic carbon, which is produced in deep layers by remineralization of exported organic carbon. The latter effect was suggested by Copin-Montégut and Bégovic (2002), who reported high values of CO_2 fugacity, and episodes of oversaturation of CO_2 with respect to atmospheric equilibrium during winter wind gusts at the DYFAMED deep station (Figure 1). Our coupled simulation does not represent the dynamics of dissolved inorganic carbon, and therefore only shows the initial effect of increasing OC export. According to Körtzinger et al. (2008) in the North Atlantic, the physical supply of dissolved inorganic carbon could have a significant effect on carbon drawdown: between 40 and 45% of the organic carbon produced during the stratified period could be respired and reinjected into the surface layer during winter mixing. Palevsky and Quay (2017) estimated this physical supply to be 40 and 90% of exported organic carbon at two sites in the North Pacific. By including this mixing-induced carbon supply in their budget, Palevsky and Quay (2017) found that carbon sequestration efficiency was lower in regions where the mixed layer was deeper.

The results of our model show that export rate and transfer efficiency at 800 m were higher in the Deep Convection region than in the shallower mixing regions. However, deep transfer and its efficiency calculated at the depth of the annual maximum mixed layer (depth corresponding to the maximum between 800 m and the local annual maximum MLD, see section 2.3) were poorer in the Deep Convection region than in the two other regions (Table 1). Indeed, in the Deep Convection region, deep transfer was much lower below the annual maximum MLD than at 800 m (5 and 45 times for POC and DOC, respectively). Efficiency of deep export and transfer calculated at the annual maximum MLD represents 11 and 17%, respectively, of deep export and transfer efficiency calculated at 800 m. In an area corresponding to one sixth of the region surface, the mixed layer reached the seabed, and OC export only corresponded to the deposition of POC. Moreover, the proportion of POC and DOC exported below the annual maximum MLD during the main convection event falls to 17 and 5% (versus 50 and 66% at 800 m), respectively, of the annual export.

However, two key characteristics of the hydrodynamics in this area suggest that this latter assessment underestimates the amount of carbon exported under the euphotic layer and isolated from the atmosphere on a decadal timescale. First, the depth of the mixed layer and the extension of the convection zone show a high interannual variability in this region (Houpert et al., 2016, for instance, they reported that the area of low surface chlorophyll ($<$0.25 mg m^{-3}), considered as a proxy of the deep convection zone, ranged between 1.5 and 56.3 km^2 between 2007/2008 and 2012/2013). Notably, according to Somot et al. (2016), the year 2012/2013 was one of the strongest convective years in the period 1980–2013. Conversely, convection was probably low in 2013/2014 (owing to the especially low heat losses in ECMWF fields), suggesting that most of the material exported below 800 m in 2012/2013 would not have been transferred back in the surface (at least in 2014), and indicating an additional vertical deep transfer through POC sedimentation. Second, the results of our model show a loss of organic carbon in the intermediate (150–800 m) and deep layers (800 m seabed) by lateral transport during and after convection periods (an amount corresponding to 20 and 45% of the OC exported during convective periods was laterally exported from the Deep Convection area into intermediate and deep layers, respectively, between February and May 2013). Concomitant with this loss in the Deep Convection region, a gain of OC in the Stratified region suggests that the OC that is transferred to deep waters by convective events in the northern region could be transported to the southern region. This is consistent with the results of Ulses et al. (2016) who calculated a north-south transfer corresponding to 53% of the OC exported below 100 m, based on the same coupled model. Moreover, this north-south transfer of OC in deep waters was suggested by Zúñiga et al. (2007) who reported higher POC fluxes at 2,145 m than at 1,440 m, based on sediment trap measurements. Our results are also consistent with the study of Schroeder et al. (2016), who demonstrated that deep dense waters formed during convective events in the northwestern region propagate throughout the western Mediterranean Sea and toward the Atlantic Ocean. It is likely that these deep waters contain carbon that was exported during convection episode, which then escapes from a transfer back to the surface layer in the following convective winters.

Finally, these findings suggest that multiannual simulations that include the dynamics of dissolved inorganic carbon are necessary to more accurately estimate the impact of convection processes on the uptake of atmospheric CO_2, and to compare the net efficiency of the three studied regions regarding this uptake.

6. Conclusion

A 3-D high-resolution coupled hydrodynamic-biogeochemical model was used to study phytoplankton dynamics and biogeochemical and physical carbon fluxes in three distinct regions of the western

Mediterranean Sea. These three regions were characterized by deep convection, shallow convection, and shallow mixing during winter. Comparisons of the results of the model with ocean color satellite observations presented here, and with in situ data presented in Kessouri et al. (2017), showed that the model correctly represented the evolution over time of chlorophyll in the three investigated regions.

The model confirms that regimes similar to subpolar and subtropical regimes coexist in the western Mediterranean Sea, within a distance of several hundreds of kilometers, in response to contrasting winter mixing conditions (Figure 9). Although this has already been established from the annual surface chlorophyll cycle, here we confirm it, based on a broader description of the functioning of the planktonic ecosystem.

The conditions of bloom onset do not significantly differ from those already described in other regions. However, in the case of the autumn bloom, we found that an increase in surface chlorophyll did not correspond to bloom onset, but rather to the erosion of the DCM. In the case of the specific period studied here, the "real" bloom (corresponding to an increase in integrated biomass) occurred 1 month later, when the mixed layer reached the nutricline. The winter/early spring bloom, as it is known in the North Atlantic, was only identified in the Deep Convection region. The processes triggering this bloom correspond to earlier descriptions of subpolar regions, with the first condition being the breakdown of turbulence. In the northwestern convection region, we identified the importance of restratification, due to baroclinic instabilities that developed rapidly after the change in sign of surface heat fluxes. This process thinned the mixed layer. This indicates that the difference between the active mixed layer (corresponding to a period of surface heat losses) and the passive mixed layer (after the change in sign of heat fluxes) is not relevant in explaining the breakdown of turbulence. This is at least true at the periphery of the convective zone, which was rapidly affected by frontal instabilities. As expected, the low grazing pressure brought about by convection through dilution allowed the explosion of the bloom.

NPP differences between the stratified and convective regions were considered insignificant because of opposing biases in the simulated surface chlorophyll in these regions. In deep convection regions, the inhibition of winter productivity during the 2 month period of the deep mixed layer contributed to reduce primary production. In contrast to annual primary production, annual export of organic carbon and its deep transfer were very different in convective and stratified regions in 2012/2013. Deep convection produced an export of particulate organic matter that was 3.5 (2.3) times higher than in the stratified region below 150 (800) m, while for total (particulate + dissolved) organic carbon, this ratio reached 5.0 (8.0) below 150 (800) m. The consequence of the two points described above is that export efficiency (export/primary production) was much higher in convective regions than in the stratified region. This is largely the result of the mixed layer pump process described by Dall'Olmo et al. (2016), which transports POC and DOC to great depths in winter. These results suggest that the higher amount of organic matter transferred to deep waters, and representing a food source for marine organisms, may make the northwestern Mediterranean convection areas a favorable habitat for the mesopelagic ecosystem. Furthermore, they highlight the importance of monitoring convective regions, as they may be modified in response to climate warming, supporting the development of a regime similar to the subtropical regime with a lower deep transfer rate.

Our analysis, which relied mainly on vertical mixing, did not investigate the coupling between different regions of the Mediterranean that, in the long term, governs the spatial distribution of nutrients. Thermohaline circulation produces a rather complex circulation of the different water masses. In the context of the present paper, Atlantic waters flow into the Algerian subbasin, and a part of them reaches then the Gulf of Lions convection zone taking a cyclonic path through the western basin. The deep waters formed in the Gulf of Lions are dispersed toward the Algerian subbasin and feed the deep waters of the western basin. Finally, the Levantine intermediate waters link the eastern and western basins. Formed in the Rhodes gyre in the Levantine basin, they collect organic matter sinking from the surface, which is recycled into nutrients (Crise et al., 1999), part of which is ultimately exported to the Atlantic. During convection in the Gulf of Lions, the nutrients transported in intermediate waters are mixed over the water column and fuel the nutrient pool of surface and deep waters. We have seen that convection exports organic matter. Although some of the exported material will be injected back into the surface layer during the next convection event, a consequence of deep circulation is horizontal transport of organic matter toward the Algerian basin. In this context, our results are in agreement with the quantification of Ulses et al. (2016), who found the transfer to the Algerian subbasin deep waters (100 m seabed) was equivalent to 53% of the OC exported below 100 m in the convective region (337×10^4 tC yr^{-1}). An additional 165×10^4 tC yr^{-1} was conveyed in the first

100 m. These advective processes are thought to create a coupling between the three regions, and their consequences, notably on carbon sequestration deserve more attention.

To conclude, it is worth restating that the results presented in the present study relate to 1 year, characterized by strong convection in the northwestern Mediterranean. This is supported by the work of Somot et al. (2016, from a model), Mayot et al. (2017b, from satellite chlorophyll), and Herrmann et al. (2017, from an analysis of altimetry and surface chlorophyll). These results should be revisited on an interannual basis, when convection is variable. Ulses et al. (2016) found that during mild winters, surface chlorophyll in the deep convection area increases almost constantly from January to mid-March. The authors also found low interannual variability in primary production (∼4%), and a POC and DOC export at 100 m of about 2 times higher for years with strong convection than with weak convection. The differences found in our study between the Deep Convection region and the two other regions are generally consistent with these results, and support the argument that the depth of the mixed layer plays a major role in the control of phytoplankton dynamics.

Acknowledgments
This study has been funded by the PERSEUS project (European Union FP7 grant Agreement 287600). It is a contribution to the MerMex (Marine Ecosystem Response in the Mediterranean Experiment) project of the MISTRALS international program. Numerical simulations were performed using the computing cluster of Laboratoire d'Aérologie and HPC resources from CALMIP grants (P1325, P09115, and P1331). We thank two anonymous reviewers for constructive comments. We thank NASA for providing surface chlorophyll data (10.5067/NIMBUS-7/CZCS/L3B/CHL/2014).

References

Allen, J. I., Somerfield, P. J., & Siddorn, J. (2002). Primary and bacterial production in the Mediterranean Sea: A modelling study. *Journal of Marine Systems*, *33–34*, 473–495. https://doi.org/10.1016/S0924-7963(02)00072-6

Anderson, T. R., & Pondaven, P. (2003). Non-redfield carbon and nitrogen cycling in the Sargasso Sea: Pelagic imbalances and export flux. *Deep Sea Research Part I: Oceanographic Research Papers*, *50*, 573–591.

Auger, P. A., Diaz, F., Ulses, C., Estournel, C., Neveux, J., Joux, F., et al. (2011). Functioning of the planktonic ecosystem on the Gulf of Lions shelf (NW Mediterranean) during spring and its impact on the carbon deposition: A field data and 3-D modelling combined approach. *Biogeosciences*, *8*(11), 3231–3261. https://doi.org/10.5194/bg-8-3231-2011

Auger, P. A., Ulses, C., Estournel, C., Stemmann, L., Somot, S., & Diaz, F. (2014). Interannual control of plankton communities by deep winter mixing and prey/predator interactions in the NW Mediterranean: Results from a 30-year 3D modeling study. *Progress in Oceanography*, *124*, 12–27. https://doi.org/10.1016/j.pocean.2014.04.004

Avril, B. (2002). DOC dynamics in the Northwestern Mediterranean Sea (DyFaMed site). *Deep Sea Research Part II: Topical Studies in Oceanography*, *49*, 2163–2182.

Baklouti, M., Faure, V., Pawlowski, L., & Sciandra, A. (2006). Investigation and sensitivity analysis of a mechanistic phytoplankton model implemented in a new modular numerical tool (Eco3M) dedicated to biogeochemical modelling. *Progress in Oceanography*, *71*(1), 34–58. https://doi.org/10.1016/j.pocean.2006.05.003

Behrenfeld, M. J. (2010). Abandoning Sverdrup's critical depth hypothesis on phytoplankton blooms. *Ecology*, *91*, 977–989.

Behrenfeld, M. J., & Boss, E. S. (2014). Resurrecting the ecological underpinnings of ocean plankton blooms. *Annual Review of Marine Science*, *6*, 167–194.

Ben Rais Lasram, F., Guilhaumon, F., Albouy, C., Somot, S., Thuillier, W., & Mouillot, D. (2010). The Mediterranean Sea as a 'cul-de-sac' for endemic fishes facing climate change. *Global Change Biology*, *16*, 3233–3245. https://doi.org/10.1111/j.1365-2486.2010.02224.x

Bentsen, M., Evensen, G., Drange, H., & Jenkins, A. D. (1999). Coordinate transformation on a sphere using conformal mapping. *Monthly Weather Review*, *127*, 2733–2740.

Bernardello, R., Cardoso, J. G., Bahamon, N., Donis, D., Marinov, I., & Cruzado, A. (2012). Factors controlling interannual variability of vertical organic matter export and phytoplankton bloom dynamics–A numerical case-study for the NW Mediterranean Sea. *Biogeosciences*, *9*, 4233–4245. https://doi.org/10.5194/bg-9-4233-2012

Bethoux, J. P. (1989). Oxygen consumption, new production, vertical advection and environmental evolution in the Mediterranean Sea. *Deep Sea Research Part A: Oceanographic Research Papers*, *36*(5), 769–781. https://doi.org/10.1016/0198-0149(89)90150-7

Bishop, J. K. B., Conte, M. H., Wiebe, P. H., Roman, M. R., & Langdon, C. (1986). Particulate matter production and consumption in deep mixed layers—Observations in a warm-core ring. *Deep Sea Research Part A: Oceanographic Research Papers*, *33*, 1813–1841.

Bosc, E., Bricaud, A., & Antoine, D. (2004). Seasonal and interannual variability in algal biomass and primary production in the Mediterranean Sea, as derived from 4 years of SeaWiFS observations. *Global Biogeochemical Cycles*, *18*, GB1005. https://doi.org/10.1029/2003GB002034

Brody, S. R., & Lozier, M. S. (2015). Characterizing upper-ocean mixing and its effect on the spring phytoplankton bloom with in situ data. *ICES Journal of Marine Science*, *72*, 1961–1970. https://doi.org/10.1093/icesjms/fsv006

Brody, S. R., Lozier, M. S., & Dunne, J. P. (2013). A comparison of methods to determine phytoplankton bloom initiation. *Journal of Geophysical Research: Oceans*, *118*, 2345–2357. https://doi.org/10.1002/jgrc.20167

Buesseler, K. O. (2007a). An assessment of the use of sediment traps for estimating upper ocean particle fluxes. *Journal of Marine Research*, *65*, 345–416.

Buesseler, K. O. (2007b). Revisiting carbon flux through the ocean's twilight zone. *Science*, *316*, 567–570.

Chiswell, S. M., Bradford-Grieve, J., Hadfield, M. G., & Kennan, S. C. (2013). Climatology of surface chlorophyll *a*, autumn-winter and spring blooms in the southwest Pacific Ocean. *Journal of Geophysical Research: Oceans*, *118*, 1003–1018. https://doi.org/10.1002/jgrc.20088

Copin-Montégut, C., & Bégovic, M. (2002). Distributions of carbonate properties and oxygen along the water column (0–2000 m) in the central part of the NW Mediterranean Sea (Dyfamed site): Influence of winter vertical mixing on air-sea CO_2 and O_2 exchanges. *Deep Sea Research Part II: Topical Studies in Oceanography*, *49*(11), 2049–2066. https://doi.org/10.1016/S0967-0645(02)00027-9

Copin-Montégut, G., & Avril, B. (1993). Vertical distribution and temporal variation of dissolved organic carbon in the North-Western Mediterranean Sea. *Deep Sea Research Part I: Oceanographic Research Papers*, *40*(10), 1963–1972.

Coppola, L., Prieur, L., Taupier-Letage, I., Estournel, C., Testor, P., Lefevre, D., et al. (2017). Observation of oxygen ventilation into deep waters through targeted deployment of multiple Argo-O_2 floats in the north-western Mediterranean Sea in 2013. *Journal of Geophysical Research: Oceans*, *122*, 6325–6341. https://doi.org/10.1002/2016JC012594

Crise, A., Allen, J., Baretta, I., Crispi, J., Mosetti, G., & Solidoro, R. C. (1999). The Mediterranean pelagic ecosystemto physical forcing. *Progress in Oceanography*, *44*(1–3), 219–243.

Crispi, G., Crise, A., & Solidoro, C. (2002). Coupled Mediterranean ecomodel of the phosphorus and nitrogen cycles. *Journal of Marine Systems*, *33–34*, 497–521.

Dall'Olmo, G. J., Dingle, L., Polimene, R. J. W., Brewinn, H. & Claustre, (2016). Substantial energy input to the mesopelagic ecosystem from the seasonal mixed-layer pump. *Nature Geoscience*, *9*, 820–823. https://doi.org/10.1038/ngeo2818

D'Ortenzio, F., Lavigne, H., Besson, F., Claustre, H., Coppola, L., Garcia, N., et al. (2014). Observing mixed layer depth, nitrate and chlorophyll concentrations in the northwestern Mediterranean: A combined satellite and NO_3 profiling floats experiment. *Geophysical Research Letters*, *41*, 6443–6451. https://doi.org/10.1002/2014GL061020

D'Ortenzio, F., & Ribera d'Alcalà, M. (2009). On the trophic regimes of the Mediterranean Sea: A satellite analysis. *Biogeosciences*, *6*, 139–148. https://doi.org/10.5194/bg-6-139-2009

Durrieu de Madron, X., Guieu, C., Sempéré, R., Conan, P., Cossa, D., D'Ortenzio, F., et al. (2011). Marine ecosystems' responses to climatic and anthropogenic forcings in the Mediterranean. *Progress in Oceanography*, *91*(2), 97–166. https://doi.org/10.1016/j.pocean.2011.02.003

Estournel, C., Testor, P., Damien, P., D'Ortenzio, F., Marsaleix, P., Conan, P., et al. (2016a). High resolution modeling of dense water formation in the north-western Mediterranean during winter 2012–2013: Processes and budget. *Journal of Geophysical Research: Oceans*, *121*, 5367–5392. https://doi.org/10.1002/2016JC011935

Estournel, C., Testor, P., Taupier-Letage, I., Bouin, M.-N., Coppola, L., Durand, J.-P., et al. (2016b). HyMeX-SOP2, the field campaign dedicated to dense water formation in the north-western Mediterranean. *Oceanography*, *29*(4), 193–206.

Gardner, W. D., Chung, S. P., Richardson, M. J., & Walsh, I. D. (1995). The oceanic mixed-layer pump. *Deep Sea Research Part II: Topical Studies in Oceanography*, *42*, 757–775.

Giering, S. L. C., Sanders, R., Martin, A. P., Henson, S. A., Riley, J. S., Marsay, C. M., et al. (2017). Particle flux in the oceans: Challenging the steady state assumption. *Global Biogeochemical Cycles*, *31*, 159–171. https://doi.org/10.1002/2016GB005424

Gogou, A., Sanchez-Vidal, A., Durrieu de Madron, X., Stavrakakis, S., Calafat, A. M., Stabholz, M., et al. (2014). Carbon flux to the deep in three open sites of the Southern European Seas (SES). *Journal of Marine Systems*, *135*, 170–179. https://doi.org/10.1016/j.jmarsys.2014.04.012

Guyennon, A., Baklouti, M., Diaz, F., Palmieri, J., Beuvier, J., Lebaupin-Brossier, C., et al. (2015). New insights into the organic carbon export in the Mediterranean Sea from 3-D modeling. *Biogeosciences*, *12*, 7025–7046. https://doi.org/10.5194/bg-12-7025-2015

Hansell, D. A., & Carlson, C. A. (1998). Net community production of dissolved organic carbon. *Global Biogeochemical Cycles*, *12*(3), 443–453. https://doi.org/10.1029/98GB01928

Helbling, E. W., & Villafañe, V. E. (2009). Phytoplankton and primary production. In *Fisheries and aquaculture* (Vol. 5, 458 p.). Encyclopedia of Life Support Systems.

Henson, S. A., Dunne, J., & Sarmiento, J. (2009). Decadal variability in North Atlantic phytoplankton blooms. *Journal of Geophysical Research*, *114*, C04013. https://doi.org/10.1029/2008JC005139

Henson, S. A., Sanders, R., & Madsen, E. (2012). Global patterns in efficiency of particulate organic carbon export and transfer to the deep ocean. *Global Biogeochemical Cycles*, *26*, GB1028. https://doi.org/10.1029/2011GB004099

Herrmann, M., Auger, P.-A., Ulses, C., & Estournel, C. (2017). Long-term monitoring of ocean deep convection using multisensors altimetry and ocean color satellite data. *Journal of Geophysical Research: Oceans*, *122*, 1457–1475. https://doi.org/10.1002/2016JC011833

Herrmann, M., Diaz, F., Estournel, C., Marsaleix, P., & Ulses, C. (2013). Impact of atmospheric and oceanic interannual variability on the Northwestern Mediterranean Sea pelagic planktonic ecosystem and associated carbon cycle. *Journal of Geophysical Research: Oceans*, *118*, 5792–5813. https://doi.org/10.1002/jgrc.20405

Ho, C., & Marra, J. (1994). Early-spring export of phytoplankton production in the northeast Atlantic-ocean. *Marine Ecology-Progress Series*, *114*, 197–202.

Houpert, L., Durrieu de Madron, X., Testor, P., Bosse, A., D'Ortenzio, F., Bouin, M. N., et al. (2016). Observations of open-ocean deep convection in the northwestern Mediterranean Sea: Seasonal and interannual variability of mixing and deep water masses for the 2007–2013 period. *Journal of Geophysical Research: Oceans*, *121*, 8139–8171. https://doi.org/10.1002/2016JC011857

Houpert, L., Testor, P., Durrieu de Madron, X., Somot, S., D'Ortenzio, F., Estournel, C., et al. (2015). Seasonal cycle of the mixed layer, the seasonal thermocline and the upper-ocean heat storage rate in the Mediterranean Sea derived from observations. *Progress in Oceanography*, *132*, 333–352.

Kessouri, F., Ulses, C., Estournel, C., Marsaleix, P., Severin, T., Pujo-Pay, M., et al. (2017). Nitrogen and phosphorus budgets in the Northwestern Mediterranean deep convection region. *Journal of Geophysical Research: Oceans*, *122*, 9429–9454. https://doi.org/10.1002/2016JC012665

Klein, B., Roether, W., Manca, B. B., Bregant, D., Beitzel, V., Kovacevic, V., et al. (1999). The large deep water transient in the Eastern Mediterranean. *Deep Sea Research Part I: Oceanographic Research Papers*, *46*(3), 371–414.

Koeve, W. (2001). Wintertime nutrients in the North Atlantic–New approaches and implications for new production estimates. *Marine Chemistry*, *74*, 245–260.

Körtzinger, A., Send, U., Lampitt, R. S., Hartman, S., Wallace, D. W. R., Karstensen, J., et al. (2008). The seasonal pCO_2 cycle at 49°N/16.5°W in the northeastern Atlantic Ocean and what it tells us about biological productivity. *Journal of Geophysical Research*, *113*, C04020. https://doi.org/10.1029/2007JC004347

Large, W. G., & Yeager, S. (2009). The global climatology of an interannually varying air-sea flux data set. *Climate Dynamics*, *33*, 341–364. https://doi.org/10.1007/s00382-008-0441-3

Lavigne, H., D'Ortenzio, F., Migon, C., Claustre, H., Testor, P., Ribera d'Alcalà, M., et al. (2013). Enhancing the comprehension of mixed layer depth control on the Mediterranean phytoplankton phenology. *Journal of Geophysical Research: Oceans*, *118*, 3416–3430. https://doi.org/10.1002/jgrc.20251

Lavigne, H., D'Ortenzio, F., Ribera d'Alcalà, M., Claustre, H., Sauzède, R., & Gacic, M. (2015). On the vertical distribution of the chlorophyll *a* concentration in the Mediterranean Sea: A basin-scale and seasonal approach. *Biogeosciences*, *12*, 5021–5039. https://doi.org/10.5194/bg-12–5021-2015

Laws, E. A., D'Sa, E., & Naik, P. (2011). Simple equations to estimate ratios of new or export production to total production from satellite-derived estimates of sea surface temperature and primary production. *Limnology and Oceanography: Methods*, *9*, 593–601. https://doi.org/10.4319/lom.2011.9.593

Lazzari, P., Solidoro, C., Ibello, V., Salon, S., Teruzzi, A., Béranger, K., et al. (2012). Seasonal and inter-annual variability of plankton chlorophyll and primary production in the Mediterranean Sea: A modelling approach. *Biogeosciences*, *9*, 217–233. https://doi.org/10.5194/bg-9-217-2012

Lellouche, J.-M., Le Galloudec, O., Drévillon, M., Régnier, C., Greiner, E., Garric, G., et al. (2013). Evaluation of global monitoring and forecasting systems at Mercator Ocean. *Ocean Science*, *9*, 57–81. https://doi.org/10.5194/os-9-57-2013

Ludwig, W., Bouwman, A. F., Dumont, E., & Lespinas, F. (2010). Water and nutrient fluxes from major Mediterranean and Black Sea rivers: Past and future trends and their implications for the basin-scale budgets. *Global Biogeochemical Cycles*, *24*, GB0A13. https://doi.org/10.1029/2009GB003594

Macias, D., Garcia-Gorriz, E., Piroddi, C., & Stips, A. (2014). Biogeochemical control of marine productivity in the Mediterranean Sea during the last 50 years. *Global Biogeochemical Cycles*, *28*, 897–907. https://doi.org/10.1002/2014GB004846

Mahadevan, A., D'Asaro, E., Lee, C., & Perry, M.-J. (2012). Eddy-driven stratification initiates North Atlantic spring phytoplankton blooms. *Science*, *337*(6090), 54–58. https://doi.org/10.1126/science.1218740

Manca, M., Burca, M., Giorgetti, A., Coatanoan, C., Garcia, M. J., & Iona, A. (2004). Physical and biochemical averaged vertical profiles in the Mediterranean regions: An important tool to trace the climatology of water masses and to validate incoming data from operational oceanography. *Journal of Marine Systems*, *48*(1–4), 83–116.

Maraldi, C., Chanut, J., Levier, B., Ayoub, N., De Mey, P., Reffray, G., et al. (2013). NEMO on the shelf: Assessment of the Iberia-Biscay-Ireland configuration. *Ocean Science*, *9*, 745–771. https://doi.org/10.5194/os-9-745-2013

Marsaleix, P., Auclair, F., Duhaut, T., Estournel, C., Nguyen, C., & Ulses, C. (2012). Alternatives to the Robert-Asselin filter. *Ocean Modelling*, *41*, 53–66. https://doi.org/10.1016/j.ocemod.2011.11.002

Marsaleix, P., Auclair, F., & Estournel, C. (2009). Low-order pressure gradient schemes in sigma coordinate models: The seamount test revisited. *Ocean Modelling*, *30*, 169–177. https://doi.org/10.1016/j.ocemod.2009.06.011

Marsaleix, P., Auclair, F., Estournel, C., Nguyen, C., & Ulses, C. (2011). An accurate implementation of the compressibility terms in the equation of state in a low order pressure gradient scheme for sigma coordinate ocean models. *Ocean Modelling*, *40*, 1–13. https://doi.org/10.1016/j.ocemod.2011.07.004

Marsaleix, P., Auclair, F., Floor, J. W., Herrmann, M. J., Estournel, C., Pairaud, I., et al. (2008). Energy conservation issues in sigma-coordinate free-surface ocean models. *Ocean Modelling*, *20*, 61–89.

Marty, J.-C., & Chiavérini, J. (2002). Seasonal and interannual variations in phytoplankton production at DYFAMED time-series station, northwestern Mediterranean Sea. *Deep Sea Research Part II: Topical Studies in Oceanography*, *49*(11), 2017–2030.

Mayot, N., D'Ortenzio, F., Ribera d'Alcalà, M., Lavigne, H., & Claustre, H. (2016). Interannual variability of the Mediterranean trophic regimes from ocean color satellites. *Biogeosciences*, *13*, 1901–1917.

Mayot, N., D'Ortenzio, F., Taillandier, V., Prieur, L., de Fommervault, O. P., Claustre, H., et al. (2017a). Physical and biogeochemical controls of the phytoplankton blooms in North Western Mediterranean Sea: A multiplatform approach over a complete annual cycle (2012–2013 DEWEX experiment). *Journal of Geophysical Research: Oceans*, *122*, 9999–10019. https://doi.org/10.1002/2016JC012052

Mayot, N., D'Ortenzio, F., Uitz, J., Gentili, B., Ras, J., Vellucci, V., et al. (2017b). Influence of the phytoplankton community structure on the spring and annual primary production in the North-Western Mediterranean Sea. *Journal of Geophysical Research: Oceans*, *122*, 9918–9936. https://doi.org/10.1002/2016JC012668

Miquel, J. C., Martín, J., Gasser, B., Rodriguez-y-Baena, A., Toubal, T., & Fowler, S. W. (2011). Dynamics of particle flux and carbon export in the northwestern Mediterranean Sea: A two decade time-series study at the DYFAMED site. *Progress in Oceanography*, *91*(4), 461–481. https://doi.org/10.1016/j.pocean.2011.07.018

Moutin, T., Raimbault, P., Golterman, H. L., & Coste, B. (1998). The input of nutrients by the Rhône river into the Mediterranean Sea: Recent observations and comparison with earlier data. *Hydrobiologia*, *373*, 237. https://doi.org/10.1023/A:1017020818701

NASA Goddard Space Flight Center, Ocean Biology Processing Group. (2014). Sea-viewing Wide Field-of-view Sensor (SeaWiFS) Ocean Color Data. Greenbelt, MD: NASA OB.DAAC/Goddard Space Flight Center. http://doi.org/10.5067/ORBVIEW-2/SEAWIFS_OC.2014.0

Palevsky, H. I., & Quay, P. D. (2017). Influence of biological carbon export on ocean carbon uptake over the annual cycle across the North Pacific Ocean. *Global Biogeochemical Cycles*, *31*, 81–95. https://doi.org/10.1002/2016GB005527

Pastor, L., Deflandre, B., Viollier, E., Cathalot, C., Metzger, E., Rabouille, C., et al. (2011). Influence of the organic matter composition on benthic oxygen demand in the Rhône River prodelta (NW Mediterranean Sea). *Continental Shelf Research*, *31*(9), 1008–1019. https://doi.org/10.1016/j.csr.2011.03.007

Petrenko, A., Dufau, C., & Estournel, C. (2008). Barotropic eastward currents in the western Gulf of Lion, north-western Mediterranean Sea, during stratified conditions. *Journal of Marine Systems*, *74*, 406–428. https://doi.org/10.1016/j.jmarsys.2008.03.004

Roether, W., Manca, B. B., Klein, B., Bregant, D., Georgopoulos, D., Beitzel, V. et al. (1996). Recent changes in Eastern Mediterranean deep waters. *Science*, *271*, 333–335.

Rubio, A., Barnier, B., Jorda, G., Espino, M., & Marsaleix, P. (2009). Origin and dynamics of mesoscale eddies in the Catalan Sea (NW Mediterranean): Insight from a numerical model study. *Journal of Geophysical Research*, *114*, C06009. https://doi.org/10.1029/2007JC004245

Santinelli, C., Nannicini, L., & Seritti, A. (2010). DOC dynamics in the meso and bathypelagic layers of the Mediterranean Sea. *Deep Sea Research Part II: Topical Studies in Oceanography*, *57*, 1446–1459.

Schroeder, K., Chiggiato, J., Bryden, H. L., Borghini, M., & Ben Ismail, S. (2016). Abrupt climate shift in the Western Mediterranean Sea. *Scientific Reports*, *6*, 23009. https://doi.org/10.1038/srep23009

Schroeder, K., Ribotti, A., Borghini, M., Sorgente, R., Perilli, A., & Gasparini, G. P. (2008). An extensive Mediterranean deep water renewal between 2004 and 2006. *Geophysical Research Letters*, *35*, L18605. https://doi.org/10.1029/2008GL035146

Sempéré, R., Charrière, B., Van Wambeke, F., & Cauwet, G. (2000). Carbon inputs of the Rhône river to the Mediterranean Sea: Biogeochemical implications. *Global Biogeochemical Cycles*, *14*(2), 669–681. https://doi.org/10.1029/1999GB900069

Severin, T., Kessouri, F., Rembauville, M. *et al.* (2017). Open-ocean convection process: A driver of the winter nutrient supply and the spring phytoplankton distribution in the Northwestern Mediterranean Sea. *Journal of Geophysical Research: Oceans*, *122*, 4587–4601. https://doi.org/10.1002/2016JC012664

Siegel, D. A., Buesseler, K. O., Doney, S. C., Sailley, S. F., Behrenfeld, M. J., & Boyd, P. W. (2014). Global assessment of ocean carbon export by combining satellite observations and food-web models. *Global Biogeochemical Cycles*, *28*, 181–196. https://doi.org/10.1002/2013GB004743

Siegel, D. A., Doney, S. C., & Yoder, J. A. (2002). The North Atlantic spring phytoplankton bloom and Sverdrup's critical depth hypothesis. *Science*, *296*, 730–733. https://doi.org/10.1126/science.1069174

Soetaert, K., Herman, P. M. J., Middelburg, J. J., Heip, C., Smith, C. L., Tett, P., et al. (2001). Numerical modelling of the shelf break ecosystem: Reproducing benthic and pelagic measurements. *Deep Sea Research Part II: Topical Studies in Oceanography*, *48*(14–15), 3141–3177. https://doi.org/10.1016/S0967-0645(01)00035-2

Somot, S., Houpert, L., Sevault, F., Testor, P., Bosse, A., Taupier-Letage, I., et al. (2016). Characterizing, modelling and understanding the climate variability of the deep water formation in the North-Western Mediterranean Sea. *Climate Dynamics*, 1–32. https://doi.org/10.1007/s00382-016-3295-0

Somot, S., Sevault, F., & Déqué, M. (2006). Transient climate change scenario simulation of the Mediterranean Sea for the twenty-first century using a high-resolution ocean circulation model. *Climate Dynamics*, *27*(7–8), 851–879.

Stabholz, M., Durrieu de Madron, X., Khripounoff, A., Canals, M., Taupier-Letage, I., Testor, P., et al. (2013). Impact of open-sea convection on particulate fluxes and sediment dynamics in the deep basin of the Gulf of Lions. *Biogeosciences*, *10*, 1097–1116.

Sverdrup, H. U. (1953). On conditions for the vernal blooming of phytoplankton. *Journal du Conseil / Conseil Permanent International pour l'Exploration de la Mer*, *18*(3), 287–295. https://doi.org/10.1093/icesjms/18.3.287

Taylor, J. R., & Ferrari, R. (2011). Shutdown of turbulent convection as a new criterion for the onset of spring phytoplankton blooms. *Limnology and Oceanography*, *56*, 2293–2307. https://doi.org/10.4319/lo.2011.56.6.2293

Uitz, J., Stramski, D., Gentili, B., D'Ortenzio, F., & Claustre, H. (2012). Estimates of phytoplankton class-specific and total primary production in the Mediterranean Sea from satellite ocean color observations. *Global Biogeochemical Cycles*, *26*, GB2024. https://doi.org/10.1029/2011GB004055

Ulses, C., Auger, P.-A., Soetaert, K., Marsaleix, P., Diaz, F., Coppola, L., et al. (2016). Budget of organic carbon in the North-Western Mediterranean Open Sea over the period 2004–2008 using 3D coupled physical biogeochemical modeling. *Journal of Geophysical Research: Oceans*, *121*, 7026–7055. https://doi.org/10.1002/2016JC011818

Waldman, R., Somot, S., Herrmann, M., Testor, P., Estournel, C., Sevault, F., et al. (2016). Estimating dense water volume and its evolution for the year 2012–2013 in the North-western Mediterranean Sea: An observing system simulation experiment approach. *Journal of Geophysical Research: Oceans*, *121*, 6696–6716. https://doi.org/10.1002/2016JC011694

Westberry, T. K., Williams, P. J. L. B., & Behrenfeld, M. J. (2012). Global net community production and the putative net heterotrophy of the oligotrophic oceans. *Global Biogeochemical Cycles*, *26*, GB4019. https://doi.org/10.1029/2011GB004094

Williams, R. G., & Follows, M. J. (2003). Physical transport of nutrients and the maintenance of biological production. In M. J. R. Fasham (Ed.), *Ocean biogeochemistry* (pp. 19–51). Berlin, Germany: Springer. https://doi.org/10.1007/978-3-642-55844-3_3

Zúñiga, D., Calafat, A., Sanchez-Vidal, A., Canals, M., Price, B., Heussner, S., et al. (2007). Particulate organic carbon budget in the open Algero-Balearic Basin (Western Mediterranean): Assessment from a one-year sediment trap experiment. *Deep Sea Research Part I: Oceanographic Research Papers*, *54*(9), 1530–1548.